The role of seasonality of mineral dust concentration and size on glacial/interglacial dust changes in the EPICA Dronning Maud Land ice core

Anna Wegner* (1), Hubertus Fischer (2), Barbara Delmonte (3), Jean-Robert Petit (4), Tobias Erhardt (2), Urs Ruth (1,5), Anders Svensson (6), Bo Vinther (6), Heinrich Miller (1)

(1) Alfred Wegener Institut Bremerhaven, Helmholtz-Zentrum für Polar- und Meeresforschung, Am Alten Hafen 26, Bremerhaven, Germany

(2) Climate and Environmental Physics, Physics Institute & Oeschger Centre for Climate Change Research, University of Bern, Sidlerstr. 5, Bern, Switzerland

(3) DISAT – Department Environmental Sciences, University Milano Bicocca, 20126, Milan, Italy

(4) Laboratoire de Glaciologie et Géophysique de l'Environnement, C. N. R. S-Université Joseph Fourier, UMR 51230, BP 96, 38402, St Martin d'Hères Cedex, France

(5) Robert Bosch GmbH, Corporate Sector Research and Advance Engineering, Renningen, 70465 Stuttgart, Germany

(6) Centre for Ica and Climate, Niels Bohr Institute, University of Copenhagen Juliane Maries Vej 30, DK-2100 Copenhagen, Denmark

* corresponding author: anna.wegner@awi.de

Key Points:

Dust concentration and size are analysed in the EDML ice core.

Seasonal phase-lag between dust concentration and size changes over Termination 1

Major atmospheric change over Antarctica likely around 16,000 yr BP

Abstract

We present a record of particulate dust concentration and size distribution in subannual resolution measured on the EPICA Dronning Maud Land (EDML) ice core drilled in the Atlantic sector of the East Antarctic plateau. The record reaches from present day back to the penultimate glacial until 145,000 yr BP with subannual resolution from 60,000 yr BP to present. Mean dust concentrations are a factor of 46 higher during the Glacial (~850-4600 ng/mL) compared to the Holocene (~16-112 ng/mL) with slightly smaller dust particles during the Glacial compared to the Holocene and with an absolute minimum in the dust size at 16,000 yr BP. The changes in dust concentration are mainly attributed to changes in source conditions in southern South America. An increase in the modal value of the dust size suggests that at 16,000 yr BP a major change in atmospheric circulation apparently allowed more direct transport of dust particles to the EDML drill site. We find a clear in-phase relation of the seasonal variation in dust mass concentration and dust size during the Glacial ($r(conc,size) = 0.8$) but no clear phase relationship during the Holocene ($0 < r(conc,size) < 0.4$). With a simple conceptual 1D-model describing the transport of the dust to the ice sheet using the size as an indicator for transport intensity, we find that the effect of the changes in the seasonality of the source emission strength and the transport intensity on the dust decrease over Transition 1 can significantly contribute to the large decrease of dust concentration from the Glacial to the Holocene.

Keywords: EPICA DML ice core, dust concentration and size, atmospheric dynamics

1. Introduction

Since Antarctica is covered to 98% by ice, the aeolian dust deposited on the Antarctic ice sheet is almost solely of remote origin and was transported thousands of kilometres in the

53 atmosphere. Accordingly, mineral dust measured in Antarctic ice cores presents a unique
54 archive to reconstruct the aeolian mineral dust load in the Southern Ocean region and
55 atmospheric dust transport to Antarctica during the past up to 800,000 years [*Lambert et al.*
56 2008, *Lambert et al.*,2012]. Previous studies showed that the dust concentration in the ice
57 cores from the East Antarctic plateau (EAP) changes on glacial-interglacial timescales by a
58 factor of approximately 50 [e.g. *Fischer et al.,* 2007a, *Lambert et al.,* 2008, *Delmonte et al.,*
59 2008, *Petit et al.,* 1999], with significant impact on the radiative balance of the Earth at least
60 on a regional scale [e.g. *Mahowald et al.,* 2003].
61
62 The dust concentration in ice cores is influenced by the conditions at the source, where the
63 dust particles are uplifted into the atmosphere, by the transport processes through the
64 atmosphere from the source to the ice sheet and by deposition processes onto the snow
65 surface. However the contribution of each of these factors to the overall glacial-interglacial
66 change is not sufficiently quantified, although different explanations are put forward [e.g.
67 *Petit and Delmonte,* 2009, *Fischer et al.,* 2007a] as summarized in the Discussion. Moreover,
68 dust enabled atmospheric circulation models still fail to reproduce the large glacial-
69 interglacial amplitudes in dust concentration variability in Antarctic ice cores by one order of
70 magnitude [e.g. *Mahowald et al.,* 2011].
71
72 Due to the purity of the ice and the small amount of sample available, the measurement of
73 dust characteristics is challenging, thus, most of the studies are based on samples with a
74 resolution of several years or decades. However, the seasonal variability of dust input to
75 Antarctica is highly variable and a different seasonal timing of source emissions and transport
76 intensity may play a significant role also in the observed long-term changes and cannot be
77 assessed with multi-year averages. Dust plumes originating from South America were found
78 in Antarctica within 6-10 days after the dust emission event [*Gasso et al.*, 2010]. But dust

79 transported in the high troposphere can have a much longer transport time to Antarctica. Due
80 to the relatively short lifetime of mineral dust aerosol of a few days to weeks, maximum dust
81 concentrations in Antarctica can only be encountered when strong source emissions and
82 efficient transport work together seasonally. There are few studies dealing with dust
83 concentration records in seasonal resolution providing information on the seasonal dust
84 concentration maximum. These studies do not give a consistent picture for the whole
85 Antarctic continent. *Bory et al.* [2010], find a maximum in dust concentration in
86 spring/summer on top of Berkner Island. At Law Dome, elevated concentrations were found
87 in spring and autumn with a minimum in winter [*Burn-Nunes et al.,* 2011]. At the northern tip
88 of the Antarctic peninsula on James Ross Island, concentrations in aluminosilicate dust levels
89 are highest during late winter [*McConnell et al.,* 2007]. Again, aerosol measurements at
90 South Pole show a dust concentration peak in austral summer [*Tuncel et al.,* 1989]. Model
91 results of seasonal dust input to all Antarctic sites suggest a maximum in summer for current
92 climate conditions [*Albani et al.,* 2012b]. These discrepancies indicate that models seem not
93 to capture the seasonality of the dust maximum very well at all Antarctic sites and that the
94 dust maxima do not occur synchronously over the whole Antarctic continent. Dust sources,
95 the dynamics of the transport and processes en route can differ significantly within Antarctica,
96 especially between lower altitude coastal sites and sites on the EAP.
97 The predominant dust source for the interior EAP during glacial times is southern South
98 America with possible inputs from additional sources during the dusty glacials [e.g. *Delmonte*
99 *et al.,* 2008, *Delmonte et al.*, 2010, *Marino et al.,* 2009]. During the Holocene, other sources
100 like Australia might become relatively more important in the Indian sector of the EAP [e.g.
101 *Revel-Rolland et al.,* 2006], whereas in the Atlantic sector the influence of Australian dust is
102 minor [*Wegner et al.,* 2012]. At the present day the emission strength of the South American
103 source is highly variable but shows a maximum in summer [*Johnson et al.,* 2010]. Also the

104 highest frequency of dust storms in Australia occurs in spring to summer [*Ekström et al.,*
105 2004].
106
107 Additional information primarily on dust transport and deposition may be derived from size
108 distribution measurements on Antarctic ice cores. Assuming a relatively constant dust size
109 during the dust emission at the source [*Kok et al.,* 2011], the dust size in the airborne mineral
110 dust aerosol is mainly influenced by the size fractionating dry deposition en route and, thus,
111 by the length of the transport time as well as transport pathways and therewith atmospheric
112 conditions. But size fractionation during the deposition process over the ice sheet may also
113 influence the size distribution in polar ice [*Unnerstad and Hansson,* 2001]. The longest record
114 of dust size from the EPICA Dome C ice core and the record from Komsomolskaya ice core
115 revealed smaller sizes during cold stages [*Lambert et al.,* 2008, *Delmonte et al.,* 2004]. This
116 was tentatively explained by changes in the contributions of dust transported over different
117 pathways, larger particles transported by advection in lower altitudes and smaller particles
118 transported in higher altitudes via subsidence [*Lambert et al.,* 2008, *Delmonte et al.,* 2004].
119 At Dome C also a slight decrease could be observed in the early deglaciation until 16,000 yr
120 BP. In the Dome B ice core the dust size record shows the opposite glacial/interglacial trend
121 with significantly larger dust particles during the glacial, which could be explained by
122 regional atmospheric circulation changes over Antarctica [*Delmonte et al.*, 2004].
123
124 For previous Antarctic ice core studies no consideration has been made that the size
125 distribution of the dust deposited on the ice sheet is not only dependent on the size
126 distribution in the overlying atmosphere (this size distribution is controlled by transport
127 intensity), but that also the ratio of wet vs. dry deposition at the site can have an influence on
128 the size of the dust deposited on the ice sheet. Generally, it is assumed that wet deposition is
129 at first order not size-fractionating, while dry deposition velocity by gravitational settling

assuming Stokes settling is dependent on the diameter squared of the dust particles. However, precipitation still has an effect on the size distribution of the deposited aerosol because the amount of wet-deposited aerosol is diluting the contribution of the size fractionating dry deposition. In essence, the dust aerosol deposited on the ice sheet is shifted to larger particles than the overlying atmospheric aerosol by dry deposition, however, the shift decreases with increasing precipitation rate and hence with the amount of wet deposition of mineral dust. Thus changes in precipitation rate, as parametrized by the accumulation rate in ice cores, from one climatic condition to another may have an impact on the size distribution of the dust in the ice, which might add to or compensate for the transport time effect. For the EAP, most of the deep drilling ice core sites have lower accumulation rates than at Dronning Maud Land (DML). Thus, an effect by wet deposition might contribute more strongly in DML, whereas at sites with even lower accumulation rate wet deposition plays an even smaller role.

Seasonal variations in dust size distribution have yet not been derived from Antarctic ice cores yet. Here we fill this gap with dust size measurements on the EPICA (European Project for Ice Coring in Antarctica) ice core drilled in DML. Within EPICA two deep ice cores were drilled. The ice core drilled in DML (EDML: 75°00′S, 00°04′E, 2882 m above sea level, [*EPICA-community members*, 2006]) has a 2-3 times higher accumulation rate than the one at Dome C (EDC: 75°06′S, 123°21′E, 3233 m above sea level, [*EPICA-community members*, 2004]) and therefore provides higher resolution records down to Marine Isotope Stage 4. Moreover, it is located in the Atlantic sector of the Antarctic continent, directly downwind of the South American continent, which is the main dust source for the EAP [e.g. *Delmonte*, 2008, *Marino et al.*, 2009]. Accordingly, the EDML ice core is excellently suited for high resolution dust studies during Termination I (hereafter T1). In this paper we present the first dust particle concentration and size record from the Atlantic sector of the EAP covering the time period from 60,000 yr BP to 7500 yr BP in subannual resolution and investigate the

156 seasonal phasing of dust concentration and size, which we use as a proxy for the transport
157 intensity. Using a conceptual model we estimate the effect that a change in seasonality could
158 have on glacial-interglacial dust concentration changes.
159
160
161 **2. Methods**
162 Samples for the dust size and concentration analyses were taken using a continuous flow
163 analysis (CFA) melting device, which precluded contact of the melt water with contaminated
164 ice core surfaces [*Kaufmann et al.*, 2008, *Röthlisberger et al.*, 2000]. Two laser particle
165 detectors (LPD, Abakus, Fa. Klotz, Bad Liebenzell, Germany) were connected to the
166 meltwater flow with a flow rate of 1.6 mL/min. Data were stored every second, yielding
167 subannual resolution records in dust concentration and size covering the Holocene and back
168 to the last glacial. With one LPD only dust concentration was analysed, whereas with the
169 second LPD dust concentration and size was analysed. For the dust concentration both
170 detectors revealed the same results. Due to dispersion in the entire melt and dust detector line
171 a nominal depth resolution of approximately 0.5 cm was achieved. The entire EDML ice core
172 starting at a depth of 113 m (~1200 yr BP) was continuously analysed down to bedrock.
173 However, below ~2400 m unambiguous dating is not possible; therefore, only results above
174 this depth (corresponding to 145,000 yr BP) are used here. Some intervals could not be
175 evaluated for high resolution dust size due to the insufficient core quality in the brittle ice
176 zone interval 700-800 m (14,600 -12,000 yr BP) and in the depth interval 1258 – 1352 m
177 (35,000 – 40,000 yr BP) due to a failure of the LPD. Due to the layer thinning with depth the
178 annual layer thickness below 1710 m was generally below 1.5 cm except for two excursions
179 of thicker layers between 1800 and 1900 m (not shown). Therefore, the dust concentration
180 and size could not be reliably derived in subannual resolution below 1710 m corresponding to
181 ~60,000 yr BP. For the size calibration of the LPD, additional samples were analyzed for dust

size and concentration using a Coulter Counter Multisizer II, Beckmann-Coulter (CC). For details of the Multisizer measurements see *Delmonte et al.,* [2002]. The calibration method was adopted from *Ruth et al.*, [2003]. For each sample measured by CC, the corresponding depth interval measured using the LPD was extracted from the continuous profile. All CC samples were taken from the upper 7 cm of each meter of the core, where the CFA measurement started a new run and often the beginning was affected by contamination or missing ice. If more than 1 cm was missing in the corresponding part of the LPD profile, the sample was not used for the calibration. If in only one of the samples from CC or LPD unusual high concentrations of larger particles were found, this was treated as contamination and the samples were not used for the calibration. Finally, a set of 45 samples was available for the calibration with similar number of Holocene and Glacial samples. Beginning with the large particles (to reduce the uncertainty due to noise in the lowermost channels), the number size distribution from the LPD samples was shifted onto the CC spectra for each of the 45 calibration samples. To this end, the bin boundaries of the LPD were adjusted to match the size distributions to the CC results (Figure 1). On the basis of the new bin boundaries a new calibration line was generated for each of the samples. Possible differences in recovery were corrected by the ratio of the concentration measured by both methods. Eventually, the new calibration line was calculated as the mean value of all 45 individual calibration lines. Examples for the Holocene (580 m) and the Glacial (1051 m) are given in Figure 1.

As a proxy for the dust size, the coarse particle percentage (CPP) was calculated by dividing the volume fraction >2 µm (diameter of a sphere with the same volume as the respective particle) by the total volume concentration (>1 µm). In previuos studies the fine particle percentage (FPP volume fraction 1µm to 2 µm devided by total volume concentration) was widely used [*e.g. Lambert et al.* 2008], which is the inverse of the CPP. For convenience, we use the CPP, as the value of both CPP and mode increase if more large particles are found in the sample. The uncertainty of the CPP inferred from the counting error of each size bin is

usually below 1%. Therefore, we can exclude, that the observed variations are caused by analytical biases. Additionally, for the low resolution profiles (1 m averages), we used the modal value μ of a fitted logarithmic normal function as a measure for the mean dust size. The uncertainty of the modal value μ is controlled by the counting error of each size bin ($\sqrt{N}$) and the interval chosen for fitting. The influence of the counting statistics was determined by a Monte Carlo technique as follows: 1000 size spectra were calculated, where the counts in each size bin were varied within the counting uncertainty. The mean of the 1000 values for this size bin equaled the measured value *N(r)* for the specific size bin and the 1σ interval the statistical counting error $\sqrt{N(r)}$ for this size bin with mean radius *r*. This was done for all size bins yielding 1000 size spectra. The mode obtained by performing a log-normal fit on all those spectra varied within 1σ of less than 0.02 μm for the glacial samples and 0.05 μm for interglacial samples. The influence of the interval chosen for fitting (approximately from 1 - 4 μm) was determined by changing the fitting interval. The range for reasonable values for μ by changing the range of the fitting interval was 0.05 μm for glacial and interglacial values and thus the dominant error compared to the counting error. For the high resolution dust size measurements, the total number of counted dust particles was often too low to fit a logarithmic normal function and the CPP provided a more robust estimate of changes in dust size. The two different size parameters are interchangeable especially during the Glacial and the first part of the transition (Figure 2 and Figure 3). Thus, the use of either of them will not affect the results and the discussion. For the Holocene the CPP appeared to be the more robust parameter. Below 2050 m (corresponding to about 87,000 yr BP) mm-scale z-folds and up to 15° tilts start to show up in visible layers in the ice core [*Faria et al.*, 2010]. At that depth CPP and mode start to diverge. Thus we assume, that dust size cannot be reliably reproduced with our methods in this depth interval and the size data are not used here. The concentration does not seem to be affected as shown by the very good correspondence of Ca^{2+} and dust concentration profiles (Figure 2). In the following we will always refer to the

234 CPP. The age scale of the EDML ice core was adopted from AICC2012 [*Veres et al.*, 2013].
235 For the depth intervals 450 – 800 m and 1450-1500 m individual layer counting was
236 conducted. For all other depth intervals the AICC2012 agescale was linearly interpolated on 1
237 m intervals.
238
239 **3. Results**
240 An overview over the dust concentration, flux and size in the EDML ice core is shown in
241 Figure 2. Additionally, accumulation rates [*EPICA-community members*, 2006], $\delta^{18}O$ values
242 [*EPICA-community members*, 2006] as an indicator for temperature, and nss-Ca^{2+}-fluxes for
243 EDML and EDC quantified using CFA [*Kaufmann et al.*, 2010] as a proxy for the soluble
244 dust fraction are given. Here, the dust particle number and dust mass concentrations are given.
245 Mass concentration and number concentration profiles show a very high coherence (Figure 2
246 (f) and (g)). Further on, only dust mass concentrations will be used (which can be directly
247 compared to other geochemically important dust tracers such as Ca^{2+}) and denoted as dust
248 concentration. The complete undisturbed ice core record reaches back to 145,000 yr BP.
249 Below that, unambiguous dating is not possible at the present stage. Down to 60,000 years the
250 annual layer thickness is above 1.5 cm, the limit for the identification of a seasonal signal.
251 Below 1.5 cm, dispersion in the CFA system does not allow to distinguish single years.
252 Accordingly, we will interpret seasonal cycles in dust concentration and size only for the last
253 60,000 years in this study.
254
255 Clearly identifiable are the strongly elevated dust levels during the Glacial stage. The mean
256 glacial dust concentration is 46 times higher than during the Interglacials (Holocene 7000 yr
257 BP – 10,000 yr BP: 16-112 ng/mL, Glacial 18,000 yr BP – 26,000 yr BP: 850-4600 ng/mL).
258 However, the absolute minimum of 6 ng/mL in the dust concentration record is reached at
259 ~11,600 yr BP. This is in line with dust concentration ratios of other Antarctic ice cores like

Vostok and EPICA Dome C [*Lambert et al.*, 2008, *Petit et al.*, 1999]. In the very low accumulation areas of the high EAP dry deposition of dust aerosol prevails. In this case variations in the dust flux are more representative of accompanying changes in the atmospheric aerosol concentration [*Fischer et al.*, 2007b]. The absolute dust flux in the EDML ice core is about twice as high as at EPICA Dome C due to the closer proximity of the EDML drill site to Southern South America (Figure 2(d)), the main glacial dust source for the entire EAP and also the predominant Holocene source in the case of EDML [*Wegner et al. 2012*]. The glacial dust flux at EDML is a factor of 18 higher than in the Holocene. The profiles of the dust concentration and the nss-Ca^{2+} concentration show very good correspondence especially for the parts of the records with higher dust concentrations, where the Ca^{2+} concentration is dominated by input of crustal material.

The dust particle size (given as modal value μ or CPP in Figure 2(c) and 3(d)) is slightly larger during the Holocene than during the Glacial. However, early during T1, the particle size intermittently decreases even further until about 16,000 yr BP, followed by an increase to the Holocene level. This is in line with results from other Antarctic ice cores. In the EPICA Dome C and Komsomolskaya ice cores, larger particles were also found during warm stages [*Delmonte et al.*, 2004]. An evident size minimum during the early deglaciation until 16,000 yr BP was also observed at Dome C [*Delmonte et al.*, 2004] and at Talos Dome [*Albani et al.,* 2012a]. For the last Glacial, there is no clear correspondence between particle size and temperature or dust concentration. Dust size in the Dome B record shows the opposite glacial/interglacial trend with significantly larger dust particles during the glacial. This has been attributed to regional differences in atmospheric pathways in terms of transport through either advection or subsidence over the EAP [*Delmonte et al.*, 2004]. Note, that when considering multi-annual mean modal values, the results are biased to the modal values occurring during the dust concentration maxima. Thus a different seasonality in dust concentration and size at different sites may also contribute to the differences in the size

record additional to the effect of different atmospheric pathways. It cannot be ruled out, that during different climatic stages, the contribution of particles transported in lower atmospheric levels by advection onto the plateau and particles transported in higher atmospheric levels and subsidence may have changed on seasonal scale. However, due to the lack of seasonally resolved dust size information at other sites, the extent of this effect cannot be quantified at this point.

The high resolution concentration and size profiles measured in this study allow for the first time also an investigation of the seasonal phase relationship of dust concentration and dust size. Examples for high reso lution size and dust mass concentrations in different climatic stages are given in Figure 4. Here, higher covariance of dust concentration and size can be identified during the Glacial compared to the Holocene. Figure 5 shows the mean seasonality during a time interval of ~3000 years during the Holocene (6700 – 9500 yr BP) and Glacial (45,000 – 48,000 yr BP). During the Glacial, CPP and dust concentration show their maximum approximately during the same time of the year, whereas during the Holocene the maximum of the CPP is opposite to the dust concentration maximum. The lower amplitude during the glacial can be explained by the lower layer thickness and therewith higher dispersion over one year. The correlation between the CPP and the dust concentration over 1 m intervals over the past 60 000 is displayed in Figure 3. To investigate the effect of the different time resolution for the Holocene and the Glacial the correlation was also calculated using data on an equidistant time scale in the depth intervals 450 - 800 m and 1450 -1500 m revealing the same results. The high correlation during the Glacial ($r = \sim 0.8$) decreases during T1 to very variable and much lower correlation coefficients between 0 and 0.4. Due to bad core quality in the so called “brittle zone”, data gaps arise between 12,000 yr BP and 16,000 yr BP. Additionally, between 35,000 yr BP and 39,000 yr BP, the dust size could not be evaluated in high resolution due to technical failure of the LPD. During Marine Isotope Stage

312 3 we find lower concentrations in parallel to the major Antarctic isotope maxima (AIM,
313 EPICA-community members, 2006). The correlation of dust concentration and CPP ranges
314 between $0.2 < r < 0.7$ for these AIM events, with lower correlations during warmer periods.
315 As mentioned above, a shift in seasonal phasing could have an influence on the multi-annual
316 mean values. During warmer climatic stages, we find more often the dust size maximum not
317 to be synchronous with the concentration maximum. The multi-annual size mean value is
318 dominated by the size during the dust maximum, thus shifted to larger particles during the
319 Glacial compared to the Holocene. The influence of the dust deposited outside the
320 concentration maximum on the multiannual mean size is much smaller. Thus, we conclude,
321 that the increase in size from the Glacial to the Holocene cannot be explained by the shift in
322 the seasonal phasing of dust concentration and size.
323
324 As mentioned above, the timing of the dust input to Antarctica during the year is not
325 simultaneous at all sites because sources, atmospheric transport dynamics and processes
326 occurring during transport can be different. To pinpoint the timing during the year when dust
327 input to DML reaches its maximum, the particle and Na^+-concentration profiles during the
328 Holocene were used. At EDML the Na^+-concentration maximum occurs clearly during austral
329 winter [*Sommer et al.*, 2000, *Weller and Wagenbach*. 2007]. In order to determine the
330 seasonality of the dust maximum at EDML, first, the maxima in the high resolution Na^+-
331 concentration profile from the EDML ice core were defined as winter and the distance
332 between adjacent Na^+-concentration maxima were subdivided in 12 equidistant intervals. The
333 position of the dust concentration maximum in one of the 12 intervals was then determined
334 (Figure 6). Note, that this plot does not show the mean seasonality, but the timing of the dust
335 peak. Dust maxima occur during all times of the year. However, most maximua are found at
336 the same time as the Na^+-concentration maximum during winter with a probability of dust
337 maximum occurrence twice as high as during summer. The analysis technique used to

338 determine Na^+-concentrations causes larger dispersion than the determination of Ca^{2+}- and
339 dust concentrations. Thus, the investigation of the phase lag of Na^+ and Ca^{2+}- as well as dust
340 concentrations cannot be performed for the deeper part at 1450 m – 1500 m, where dust
341 concentrations still show a seasonal signal, whereas seasonal variability in Na^+ - concentration
342 is completely smoothed out in the CFA data.
343
344 4. **Discussion**
345 4.1 Multiannual mean values
346 First, we will focus on the multiannual mean values of the dust proxies with emphasis on the
347 dust size. The decrease of the dust concentration during T1 starts around 20,000 yr BP (Figure
348 3). Simultaneously, also the dust size starts to decrease until ~16,000 yr BP, where a sharp
349 increase in the dust size to larger Holocene values can clearly be discerned. This intermittent
350 decrease in dust size during T1 could also be observed in Dome C and Talos Dome [*Delmonte*
351 *et al.*, 2004, *Albani et al.*, 2012a]. At the same time, the chemical signature of the dust
352 changes in DML and Dome C [*Röthlisberger et al.*, 2002, *Gabrielli et al.,* 2010, *Wegner et*
353 *al.*, 2012]. A divergence between the dust flux in Talos Dome and Dome C, was found after
354 16,000 yr BP with a higher ratio between Talos Dome and EDC dust fluxes after 16,000 yr
355 BP compared to the time before [*Albani et al.*, 2012b]. Summarizing the observations from
356 the Antarctic dust records, evidence increases that around 16,000 yr BP a significant change
357 occurred in either the sources or the transport characteristics of dust, that had an Antarctic
358 wide influence on the dust deposition.
359 In previous studies the glacial/interglacial decrease in the dust flux was explained by an
360 increased hydrological cycle, weaker source emissions and a change in atmospheric transport
361 [e.g. *Petit et al.*, 1999, *Fischer et al.*, 2007b]. *Röthlisberger et al.* [2002] attributes the
362 changes in dust flux during the first part of T1 (until 15,000 yr BP) mainly to changes in the
363 source areas (vegetation cover and local climate) and the further decrease to a reorganization

364 of atmospheric circulation. From a sediment core offshore Chile at 41°S an increase in sea
365 surface temperatures (SSTs) occurred mainly between 18,800 yr BP and 16,700 yr BP [*Lamy*
366 *et al.,* 2007], which is closely linked to the position of the southern westerly wind belt
367 (SWW), which has large impacts on the uplift and long range transport of dust from
368 Patagonia, the main source area until 16,000 yr BP. *Stenni et al.* [2010] observed a different
369 climatic evolution between the Atlantic and the Indo-Pacific sector between 16,000 yr BP and
370 14,500 yr BP with a deceleration of the warming in the Atlantic Sector connected to different
371 shifts in moisture sources, which is explained by a reorganization of the atmospheric
372 circulation. Taking these facts together, evidence becomes stronger that T1 can be subdivided
373 into two parts. During the first part from 20,000 yr BP until around 16,000 yr BP gradual
374 processes like a weakening of the source due a shift in the westerly wind belt cause the
375 decrease in dust concentration. Around 16,000 yr BP, a more abrupt change happened with an
376 Antarctic wide atmospheric reorganisation, that allowed more direct transport of dust
377 indicated by larger particles to DML.
378
379 The dust size is modulated by changes in transport time and pathways [*Ruth et al.*, 2003,
380 *Fischer et al.*, 2007b] as well as the snow accumulation rate through atmospheric scavenging
381 processes. The significant warming between 18,000 and 16,000 yr BP and further on during
382 the transition suggests also an increasing accumulation rate at this time [*EPICA-community*
383 *members*, 2004, 2006], which would favor smaller particles in the ice at the onset of the
384 termination. This is suggested by the dust size change in Figure 3, however, the change in the
385 accumulation rate, which is significantly less than a factor of 2 at this point, cannot
386 quantitatively explain the accompanying decrease in dust concentration of about a factor of
387 10. Additionally, the dust size starts to decrease already at 20,000 yr BP whereas the increase
388 of accumulation rate seem to start slightly later. Thus especially during the time between
389 20,000 yr and 18,000 yr BP accumulation rate changes probably does not account for a

390 reduction in dust size. Alternatively, a less efficient transport at the onset of the termination
391 could contribute to the smaller particles at that time and would also slightly reduce the dust
392 concentration. However, the main driver of the 10-fold decrease in dust concentration in this
393 time interval appears to be a reduction in source strength.
394 After 16,000 yr BP the dust concentration continues to decrease but the dust size is
395 increasing. This occurs at a time where accumulation rates continue to rise significantly and,
396 thus, we can exclude that accumulation rate accounts for the change in dust size. At that time
397 the transport effect must overcompensate a reduced relative contribution of size fractionating
398 dry deposition and we conclude that after 16,000 yr BP transport must have intensified or
399 different transport pathways enabling larger particles to reach DML became more important.
400 This explanation holds both for EDML, EDC and Komsomolskaya but cannot explain the
401 opposite glacial/interglacial change of dust size at Dome B. The latter may reflect a regional
402 difference in dust transport [*Delmonte et al.*, 2004]. A more efficient transport for dust to the
403 EAP during the second part of the transition, however, would also lead to higher dust
404 concentrations. This may be partly compensated by the stronger wash out of particles en route
405 reducing the atmospheric life time of dust and the higher snow accumulation at that time
406 leading to a dilution of dust concentrations in the ice. Also, a decrease in the source strength
407 occurring simultaneously could lead to a decreased dust concentration in the ice. If the
408 accompanying change in Rare Earth element composition at ~16,000 yr BP [*Wegner et al.,*
409 *2012*] is due to a strong reduction of one source, this supports the latter explanation. The total
410 change in dust concentration after 16,000 yr BP to the Holocene is a decline by a factor of 4-
411 5, which is in the possible range of the combined effects on dust concentration by stronger
412 wet deposition during transport and at the ice core drill sites (see also section on seasonality
413 below). Interestingly, such competing effects of shortened transport time and significantly
414 reduced atmospheric lifetime are in general agreement with little net change in the difference
415 between dust fluxes between EDML and EDC over time [*Fischer et al*., 2007a], assuming a

major Patagonian dust contribution for both sites. Note, however, that for sites in the Indopacific sector of the EAP such as Dome C other sources than Patagonia become relatively more important in the late stage of the transition.

Thus we conclude that during the first part of T1 up to 16,000 yr BP, where only South American dust is identified in East Antarctica, a reduced emissivity of the source must have occurred accompanied by a less effective transport. Additionally an increase of wet deposition could have played a minor role. After 16,000 yr BP the source strength may have continued to decline but a reorganization of atmospheric circulation allowed for faster dust transport or different transport pathways but significantly increased wash out of dust during transport.

4.2 High resolution dust concentration and size profile

Quantitatively disentangling the contribution of different processes to the large glacial/interglacial variability in dust concentration in ice cores is a key question. Here we propose a new approach using subannual resolution dust concentration and size profiles to investigate possible seasonal processes contributing to the decrease in dust flux over T1:

The main processes influencing the dust concentration in the snow C_{snow} for different time periods (t1 and t2) are the source emission strength E, the transport efficiency T and processes related to the deposition D with:

$$\frac{C_{t1}}{C_{t2}} = \frac{E_{t1}}{E_{t2}} \cdot \frac{T_{t1}}{T_{t2}} \cdot \frac{D_{t1}}{D_{t2}} \quad (1)$$

Martinez-Garcia et al., [2009] found a factor of 5 higher dust fluxes in the glacials compared to interglacials in a sediment core from the South Atlantic, at a site directly downwind Patagonia, the main dust source for the EAP during Glacials [e.g. *Delmonte et al.*, 2008, *Marino et al.*, 2009, *Gabrielli et al.*, 2010] and for DML also during the Holocene [*Wegner et*

al., 2012]. Thus, this record can be taken as an estimate for the ratio in the Patagonian dust source emission strength between the last Glacial and the Holocene. *Petit and Delmonte*, [2009] derived a factor of 2-4 change in apparent source strength slightly lower than *Martinez-Garcia et al.* [2009]. Since on the EAP most of the dust is deposited by dry deposition, the increase in snow accumulation between the last glacial to the Holocene accounts for another factor of 2 in the dust concentration [*EPICA-community members*, 2006]. Overall changes in emission strength together with changes in local deposition over the ice sheet (due to the lower glacial accumulation rate) can explain about a factor of 10 (out of 46) in the glacial/interglacial dust concentration change. Accordingly, another factor of 4-5 is missing in the budget.

As outlined above the increase in dust size in the later part of the transition implies a faster or more direct transport and thus a tendency to higher concentration at that time, which is the opposite to the observed decrease in dust concentration during that time. When looking at multi-annual mean modal values, the obtained size is biased to the sizes occurring during the dust concentration maxima, which could affect the estimates for the glacial/interglacial change in dust concentration. In this study, we address the question how much of the glacial-interglacial dust concentration changes can be attributed to a change in the seasonal phasing of dust transport and dust emission. Needless to say that other processes such as a reduced hydrological cycle and the larger amount of total emitted dust during the glacial are other important factors influencing the dust concentration in Antarctic ice cores.

To explain the effect of the phase lag in dust concentration and size on the glacial/interglacial dust difference we apply a simple conceptual model for the dust transport from the dust source to the ice sheet.

Taking into account a seasonal variability in each of the components Eq. (1) turns into

$$C_{snow}(t) = E(t) \cdot T(t) \cdot D(t) \quad (2)$$

where t is the time of the year. The maximum of the dust storm frequency in Patagonia at present day occurs in summer [*Johnson et al.*, 2010]. This already shows that the occurrence of the dust maximum in EDML in winter for interglacial conditions cannot be explained by the emission seasonality E(t), but is controlled by the recent seasonality in transport and/or deposition.

To estimate a magnitude of the effect of seasonality with our simple model approach we describe the dust emission E(t) with a sin-function

$$E(t) = \Delta E \cdot \sin(\omega_E \cdot t) + \overline{E} \quad (3)$$

with $\overline{E}$ the mean total emission flux per year, $\omega_E = 2\pi / 1 year$ and *t* given in years.. ΔE accounts for the seasonal amplitude in source, with $\Delta E < \overline{E}$, to exclude a negative value for the source strength.

Based on an atmospheric model, the simulated tracer age [*Krinner and Genthon*, 2003] at the EDML drill site as a proxy for the age of the air mass reaching the site is smaller in austral winter than summer for present day and the LGM. However, the absolute modeled tracer age is smaller in the LGM compared to present day. Also backtrajectory studies [*Rejmer et al.*, 2002] show a clear seasonal cycle in transport times of air masses reaching the EAP. In this meteorological study recent transport to EDML is also slowest in austral summer and more efficient in winter, but most efficient in austral spring. In any case a significant seasonal variation in transport time for dust transport to EDML can be expected. We describe the transport with a sine function

$$T(t) = \Delta T \cdot \sin(\omega_T \cdot t + \varphi) + \overline{T} \quad (4)$$

With $\overline{T}$ the mean transport intensity during one year, $\omega_T = 2\pi / 1 year$ and $0 < \varphi < 2\pi$. ΔT accounts for the seasonal amplitude in transport efficiency, with $\Delta T < \overline{T}$, to exclude transport

489 from Antarctica to the source area. The phase $0 < \varphi < 2\pi$ accounts for the case that dust
490 emission and transport occurs at different times of the year.
491
492 Wet deposition of dust particles occurs in combination with snow accumulation, whereas dry
493 dust deposition is caused by gravitational fallout. At present day about 75% of the dust is
494 estimated to be dry deposited at DML [*Fischer et al.*, 2007b]. During the glacial, when
495 accumulation rates in DML were similar to present day Dome C accumulation, almost all dust
496 is expected to be dry deposited [Fischer et al. 2007b]. The overall higher snow accumulation
497 during the Holocene shifts the modal value of the dust volume distribution to smaller values
498 during wet deposition but does not change the seasonality in dust deposition per se. Here the
499 seasonal variation in snow accumulation and its glacial/interglacial change have to be
500 considered. For instance a higher snow accumulation in winter as suggested by [*Laepple et*
501 *al.*, 2011] will favor smaller particles to be deposited during that season. Dependent on the
502 seasonality of dust transport, the seasonal preference of larger dust particles due to changes in
503 the transport time may be either compensated or amplified by the seasonality in precipitation.
504 For present day there exist no reliable seasonally resolved precipitation measurements for the
505 EDML drill site. For other sites on the EAP higher snow accumulation rates were estimated
506 for austral winter [*Laepple et al.*, 2011 and references therein]. The snow height recorded by
507 an automatic weather station in the vicinity of the EDML drill site does not provide a picture
508 representative of the seasonality in precipitation [*Welker et al.*, 2015], but modeling studies
509 suggest that most precipitation is supplied by single snowfall events distributed randomly
510 over the year [*Reijmer and van den Broeke*, 2001, *Schlosser et al.*, 2010]. For the last glacial
511 there exists no direct estimates of the seasonality in precipitation at all for Antarctica,
512 however there is no indication for a changed seasonality compared to present day [*Laepple et*
513 *al.*, 2011]. To assess the effect of seasonality on the change in the glacial/interglacial dust
514 budget, only the change in precipitation seasonality between Glacial and Holocene has to be

515 considered. Here we assume that the seasonality in precipitation [*Laepple et al.*, 2011] and
516 thus *D(t)* has not changed over time. Accordingly, in the following we will neglect the
517 influence of changes in deposition seasonality in our model.
518
519 By using equation (2), (3) and (4) with variable φ we can describe a variable phase lag
520 between dust emission and dust transport intensity throughout the year (illustrated in Figure
521 7). For variable φ and fixed ΔT, ΔE, $\overline{T}$ and $\overline{E}$ we calculated the correlation coefficient r
522 between T and C_{snow}.
523 In the following we estimate how the phase lag between T and C influences the loss compared
524 to in-phase emission and transport. Note, however, that the results still depend on the values
525 of $\overline{E}$, $\overline{T}$ and ΔE, ΔT in Eq. (3) and (4). Figure 8 illustrates the reduction of the dust
526 concentration between source and sink solely from a changed phase-lag of dust emission and
527 transport. For aligned maxima of E(t) and T(t) ($\varphi = 0$) the reduction is 1. With increasing φ
528 the loss due to the changed phase lag increases to a minimum at $\varphi = \pi$. This implies that for
529 an out-of-phase relationship between emission and transport efficiency the high dust load at
530 the source cannot by efficiently transported to Antarctica.
531
532 For the last glacial maximum we find correlation coefficients r(CPP,C) ~ 0.8 between the dust
533 size and concentration. Taking this as an estimate for r(T,C), the corresponding value
534 $(\mathrm{E}\cdot\mathrm{T})_{\mathrm{norm}} = (\mathrm{E}\cdot\mathrm{T}(\varphi))/(\mathrm{E}\cdot\mathrm{T}(\varphi=0))$ ranges between $0.8 < (E\cdot T)_{norm} < 0.85$ dependent on $\overline{T}/\Delta\mathrm{T}$
535 corresponding to a reduction of the maximum possible $(\mathrm{E}\cdot\mathrm{T})_{\mathrm{norm}}$ to ~ 80 – 85 % (indicated as
536 horizontal and vertical dashed lines in Figure 9). For typical Holocene correlation coefficients
537 $0 < \mathrm{r(T,C)} < 0.4$, the corresponding value of $(\mathrm{E}\cdot\mathrm{T})_{\mathrm{norm}}$ ranges between $0.32 < (E\cdot T)_{norm} < 0.68$
538 dependent on $\overline{T}/\Delta\mathrm{T}$. With our conceptual model approach this corresponds to a reduction of
539 $(E\cdot T)_{norm}$ to ~32 – 50%, i.e. a factor of 2 reduction of $(E\cdot T)_{norm}$ relative to its glacial value

solely due to the dephasing of emission and transport seasonality. Note, that the higher the background transport intensity given by $\bar{T}$ the smaller is the influence of the seasonality. For $\bar{T}/\Delta T = 1$, $(E \cdot T)_{norm}$ is reduced by approximately a factor of 2 from ~0.8 to 0.32-0.5. However, for $\bar{T}/\Delta T = 1.5$, $(E \cdot T)_{norm}$ is reduced by a factor of 1.4 from ~0.85 to 0.55-0.65 between the Glacial and the Holocene.

As $(E \cdot T)_{norm}$ gives the contribution of a change in the seasonality to the observed Glacial/Interglacial dust decrease, in this simple model approach we find a possible influence of a changed seasonality between dust concentration and size of a factor of 1.5 - 2 contributing to the glacial/interglacial dust concentration in EDML change dependent on the phasing of E(t) and T(t). The maximum effect is achieved if emission and transport where in-phase during the glacial and uncorrelated in the interglacial, as suggested by our high-resolution dust data.

What causes the de-phasing of emission and transport during the transition? A contribution by other dust sources like Australia during a different season could influence our estimate. At present day the highest frequency of dust storms in Australia occurs in spring to summer [*Ekström et al.*, 2004], exhibiting only a small shift compared to the summer maximum in Southern South America. As the dust input to DML is dominated by South American dust, the minor contribution by Australian dust is not expected to change the seasonal signal in the dust record significantly. Alternatively, local sources in the Transantarctic Mountains could act as a dust supplier but mainly for larger particles. Another possible contribution to the dust input to DML could originate from the Puna Altiplano (PAP) in Bolivia. There is no study yet, that could distinguish from where in South America the dust reaching DML originates from. In the PAP most of the annual precipitation occurs during austral summer. The maximum wind speed is observed during winter and early spring, when the subtropical jet stream crosses the

PAP [*Clapperton*, 1993]. In contrast to dust emission from Southern Patagonia, this favors the dust emission in austral winter and early spring. Studies on Sr and Nd isotopes indicate that the PAP has contributed to the dust input in the Indian sector of the East Antarctic plateau as a second contributor besides the Patagonian Pampa [*Gaiero*, 2007, *Delmonte et al.*, 2008]. The proximity to DML makes it likely, that the PAP might have contributed to the dust input in DML. Thus, additional to the summer emissions from Patagonia a contribution from the PAP during winter and early spring, when dust transport intensity is strongest [*Krinner and Genthon*, 2003] or a contribution from local sources cannot be ruled out and could lead to a decorrelation of dust concentration and size. To further evaluate the possibility, if different dust sources contribute during different times of the year, provenance studies in seasonal resolution as the one performed by Bory et al. [2010] in Berkner Island are needed.

In summary we can draw the following picture of the main factors influencing the dust reaching DML during the Glacial and the Holocene: During the Glacial a longer atmospheric lifetime and stronger dust emissions lead to more dust in the atmosphere especially over the sources. Under favorable glacial conditions for intensified direct transport (indicated by larger particles) a synchronous seasonal maximum occurs in DML in dust size and concentration. During the Holocene a shorter atmospheric lifetime and a weaker source lead to a general reduction of the amount of dust in the atmosphere over the source. However, during the Holocene, favorable conditions for intensified transport (indicated by larger particles) are mostly seasonally decoupled from elevated concentrations at the source and thus no dust concentration maximum occurs in DML at the same time.

A stronger coupling between the Antarctic climate and the southern hemisphere mid-latitude climate during glacial times compared to warm stages was already proposed by *Lambert et al.* [2008]. A high atmospheric dust concentration over the source during favorable transport

conditions leads to a more direct transfer of the climatic signal from South America to Antarctica, resulting in a stronger coupling of the two regions supporting the results by *Lambert et al.* [2008]. The onset of the major deglacial decrease in dust concentration occurs simultaneously with the increase in temperature (expressed as $\delta^{18}O$ values, Figure 3) and the decrease of the correlation between dust concentration and size around 20,000 yr BP (Figure 6). This coincides with the southward displacement of the westerly wind belt [*Lamy et al.*, 1999], indicating that the westerly wind belt may have played a major role for the emission strength of the dust sources in Southern South America. In this respect the long-term changes in dust size distribution at EDML may be also partly interpreted to reflect changes in the position of the westerly wind belt.

Conclusions:

In this study we investigated for the first time the dust concentration and size in the Atlantic sector of the EAP and its seasonal phasing over the last 60,000 yr BP. We find 46 times higher dust concentrations and smaller dust particles during the LGM compared to the Holocene. In the interval 20,000 – 16,000 yr BP a reduced emissivity of the source area compared to the peak glacial and a reduction in transport intensity are identified as the main factors controlling the dust concentration decrease in Antarctic ice cores. An abrupt increase in dust size and a change in the dust provenance indicate an atmospheric reorganization at around 16,000 yr BP. Adding to previously proposed interpretations, where differences in dust sizes were explained by transport in different atmospheric altitudes [*Delmonte et al.*, 2004, 2005], we propose an additional effect acting on seasonal scale at EDML. We find a high correlation of $r = 0.8$ between dust size and dust concentration in the ice during the cold glacial and lower values with higher variability during warmer stages with $0 < r < 0.4$ during the Holocene. We argue that dust input to Dronning Maud Land is much more efficient if dust emission and favorable dust transport conditions occur at the same time of the year.

According to our study at EDML this is the case during colder climate and but not during warmer climate. Applying a conceptual model approach using the dust size as a proxy for transport we derive a contribution of a factor of 1.5-2 to the observed factor of 46 of the Glacial-Interglacial dust concentration decrease at EDML by decoupled changes in seasonality of dust emission and transport. Together with the glacial/interglacial source change estimate derived from marine records in the Atlantic sector of the Southern Ocean [*Martinez-Garcia et al.*, 2009] of a factor of 5 and a doubling of the accumulation rate from glacial to interglacial conditions (changing the total dust deposition at the drill site) this leaves a further reduction factor of 2-3 to be explained by the net change in atmospheric aerosol concentrations due to transport effects like increased washout en-route, where a shorter lifetime during warm conditions overcompensates the somewhat faster transport.

Acknowledgments:

We thank two anonymuous reviewers for usefuls suggestions to improve the manuscript. This work is a contribution to the European Project for Ice Coring in Antarctica (EPICA), a joint European Science Foundation/European Commission scientific programme, funded by the EU and by national contributions from Belgium, Denmark, France, Germany, Italy, the Netherlands, Norway, Sweden, Switzerland and the United Kingdom. The main logistic support was provided by IPEV and PNRA (at Dome C) and AWI (at Dronning Maud Land). This is EPICA publication no. 301.. The Division for Climate and Environmental Physics, Physics Institute, University of Bern acknowledges the long-term financial support of our Continuous Flow Analysis on ice cores by the Swiss National Science Foundation (SNSF). Anna Wegner thanks DGF and REKLIM for funding. Data are available on www.pangaea.de.

644 **References**

645

646 S. Albani, S., Delmonte, B., Maggi, V., Baroni, C., Petit, J.R., Stenni, B., Mazzola, C., and
647 Frezzotti, M. (2012a) Interpreting last glacial to Holocene dust changes at Talos Dome (East
648 Antarctica): implications for atmospheric variations from regional to hemispheric scales,
649 Clim. Past, 8, 741–750, doi:10.5194/cp-8-741-2012.

650

651 Albani, S., Mahowald, N.M., Delmonte, B., Maggi, V., and Winckler, G. (2012b), Comparing
652 modeled and observed changes in mineral dust transport and deposition to Antarctica between
653 the Last Glacial Maximum and current climates, Clim Dyn, doi:10.1007/s00382-011-1139-5.

654

655 Bory, A.; Wolff, E.; Mulvaney, R.; Jagoutz, E.; Wegner, A.; Ruth, U. and Elderfield, H.
656 (2010), Multiple sources supply eolian mineral dust to the Atlantic sector of coastal
657 Antarctica: Evidence from recent snow layers at the top of Berkner Island ice sheet
658 Earth Planet Sci Lett, 291, 138–148, doi:10.1016/j.epsl.2010.01.006.

659

660 Burn-Nunes, L., Vallelonga, P., Loss, R.D., Burton, G.R., Moy, A., Curran, M., Hong, S.,
661 Smith, A.M., Edwards, R., Morgan, V.I. and Rosman, K.J.R. (2011), Seasonal variability in
662 the input of lead, barium and indium to Law Dome, Antarctica, Geochim Cosmochim Ac 75,
663 1–20, doi:10.1016/j.gca.2010.09.037.

664

665 Clapperton, C. (1993), Quaternary Geology and Geomorphology of South America, 780 pp.,
666 Elsevier, Amsterdam.

667

668 Delmonte, B., Petit, J. R., and Maggi, V. (2002) Glacial to Holocene implications of the new
669 27000-year dust record from the EPICA Dome C (East Antarctica) ice core, Clim. Dynam.
670 18, 647-660, doi: 10.1007/s00382-001-0193-9.
671
672 Delmonte, B., Petit, J. R., Andersen, K. K., Basile-Doelseh, I., Maggi, V., and Lipenkov, V.
673 Y. (2004), Dust size evidence for opposite regional atmospheric circulation changes over east
674 Antarctica during the last climatic transition, Clim. Dynam., 23, 427–438, doi:
675 10.1007/s00382-004-0450-9.
676
677 Delmonte, B.; Petit, J. R.; Krinner, G.; Maggi, V.; Jouzel, J. and Udisti, R. (2005), Ice core
678 evidence for secular variability and 200-year dipolar oscillations in atmospheric circulation
679 over East Antarctica during the Holocene, Clim. Dynam., 24, 641-654, doi: 0.1007/s00382-
680 005-0012-9,
681
682 Delmonte, B., Andersson, P. S., Hansson, M., Schoeberg, H., Petit, J., Basile-Doelsch, I., and
683 Maggi, V. (2008), Aeolian dust in East Antarctica (EPICA-Dome C and Vostok): Provenance
684 during glacial ages over the last 800 kyr, Geophys. Res. Lett., 35, L07703,
685 doi:10.1029/2008GL033382.

686 Delmonte, B., Andersson, P.S., Schöberg, H., Hansson, M., Petit, J.R., Delmas, R., Gaiero,
687 D.M., Maggi, V., and Frezzotti, M., (2010) Geographic provenance of aeolian dust in East
688 Antarctica during Pleistocene glaciations: preliminary results from Talos Dome and
689 comparison with East Antarctic and new Andean ice core data, Quat. Sci. Rev., 29, 1-2, 256-
690 264, doi: 10.1016/j.quascirev.2009.05.010.

691 Ekström, M., McTainsh, G.H., and Chappell, A. (2004), Australian dust storms: temporal
692 trends and relationships with synoptic pressure distributions (1960–99), Int. J. Climatol., 24
693 (12), 1581-1599, doi: 10.1002/joc.1072.
694
695 EPICA-Community Members (2004), Eight glacial cycles from an Antarctic ice core, Nature
696 429, 623–628, doi: 10.1038/nature02599.
697
698 EPICA-Community Members (2006), One-to-one coupling of glacial climate variability in
699 Greenland and Antarctica, Nature, 444, 195–198, doi: 10.1038/nature05301.
700
701 Faria, S.; Freitag, J.; and Kipfstuhl, S. (2010), Polar ice structure and the integrity of ice-core
702 paleoclimate records, Quat. Sci. Rev. 29, 338-351, doi: 10.1016/j.quascirev.2009.10.016.
703
704 Fischer, H., Fundel, F., Ruth, U., Twarloh, B., Wegner, A., Udisti, R., Becagli, S., Castellano,
705 E., Morganti, A., Severi, M., Wolff, E., Littot, G., Röthlisberger, R., Mulvaney, R., Hutterli,
706 M. A., Kaufmann, P., Federer, U., Lambert, F., Bigler, M., Hansson, M., Jonsell, U., de
707 Angelis, M., Boutron, C., Siggaard-Andersen, M. L., Steffensen, J. P., Barbante, C., Gaspari,
708 V., Gabrielli, P., and Wagenbach, D. (2007a), Reconstruction of millenial changes in the dust
709 emission, transport and regional sea ice coverage using the deep EPICA ice cores from the
710 Atlantic and the Indian sector of Antarctica, Earth Planet. Sc. Lett., 260, 340–354,
711 doi:10.1016/j.epsl.2007.06.014.
712
713 Fischer, H.; Siggaard-Andersen, M. L.; Ruth, U.; Röthlisberger, R. & Wolff, E. (2007b)
714 Glacial/interglacial changes in mineral dust and sea-salt records in polar ice cores: Sources,
715 transport, and deposition, Rev. Geophys., 45, RG1002, doi: 10.1029/2005RG000192.
716

717 Gabrielli, P., Wegner, A., Petit, J.-R., Delmonte, B., De Deckker, P., Gaspari, V., Fischer, H.,
718 Ruth, U., Kriews, M., Boutron, C., Cescon, P., and Barbante, C. (2010), A major glacial-
719 interglacial change in aeolian dust composition inferred from Rare Earth Elements in
720 Antarctic ice, Quaternary. Sci. Rev., 29, 265–273, doi:10.1016/j.quascirev.2009.09.002.
721
722 Gaiero, D. M. (2007), Dust provenance in Antarctic ice during glacial periods: From where in
723 southern South America? Geophys. Res. Lett., 34, L17707, doi:10.1029/2007GL030520.
724
725 Gasso, S., Stein, A., Marino, F., Castellano, E., Udisti, R., and Ceratto, J. (2010) A combined
726 observational and modeling approach to study modern dust transport from the Patagonia
727 desert to East Antarctica, Atmos. Chem. Phys., 10, 8287–8303, doi:10.5194/acp-10-8287-
728 2010.
729
730 Johnson, M.; Meskhidze, N.; Solmon, F.; Gassó, S.; Chuang, P.; Gaiero, D.; Yantosca, R.;
731 Wu, S.; Wang, Y. and Carouge, C. (2010), Modeling dust and soluble iron deposition to the
732 South Atlantic Ocean, J. Geophys. Res.., 115 D15202 doi:10.1029/2009JD013311.
733
734 Kaufmann, P., Federer, U., Hutterli, M. A., Bigler, M., Schüpbach, S., Ruth, U., Schmitt, J.,
735 and Stocker, T. F. (2008), An improved Continuous Flow Analysis (CFA) system for high-
736 resolution field measurements on ice cores, Environ. Sci. Technol. 42, 8044-8050, doi:
737 10.1021/es8007722.
738
739 Kaufmann, P;, Fundel, F.;Fischer, H.; Bigler, M.; Ruth, U.; Udisti, R.; Hansson, M.; de
740 Angelis, M.; Barbante, C.; Wolff, E.; Hutterli, M. and Wagenbach, D. (2010), Ammonium
741 and non-sea salt sulfate in the EPICA ice cores as indicator of biological activity in the
742 Southern Ocean, Quat. Sci. Rev., 29, 313-323, doi: 10.1016/j.quascirev.2009.11.009.

743 Kok, J. (2011), Does the size distribution of mineral dust aerosols depend on the wind speed
744 at emission? Atmos. Chem. Phys., 11, 10149–10156, doi:10.5194/acp-11-10149-2011.
745
746 Krinner G. and Genthon, C. (2003), Tropospheric transport of continental tracers towards
747 Antarctica under varying climatic conditions, Tellus, 55B, 54-70.
748
749 Laepple, T.; Werner, M. and Lohmann, G. (2011), Synchronicity of Antarctic temperatures
750 and local solar insolation on orbital timescales, Nature, 471, 91-94, doi:10.1038/nature09825.
751
752 Lambert, F., Delmonte, B., Petit, J. R., Bigler, M., Kaufmann, P. R., Hutterli, M. A., Stocker,
753 T. F., Ruth, U., Steffensen, J. P., and Maggi, V. (2008), Dust-climate couplings over the past
754 800,000 years from the EPICA Dome C ice core, Nature, 452, 616–619,
755 doi:10.1038/nature06763.
756
757 Lambert, F., Bigler, M., Steffensen, J. P., Hutterli, M., and Fischer, H. (2012), Centennial
758 mineral dust variability in high-resolution ice core data from Dome C, Antarctica, Clim Past,
759 8, 609-623, 10.5194/cp-8-609-2012.
760
761 Lamy, F.; Hebbeln, D. and Wefer, G. (1999), High-Resolution Marine Record of Climatic
762 Change in Mid-latitude Chile during the Last 28,000 Years Based on Terrigenous Sediment
763 Parameters, Quaternary Res. 51, 83–93, doi: 10.1006/qres.1998.2010.
764
765 Lamy, F.; Kaiser, J.; Arz, H. W.; Dierk Hebbeln, D.; Ninnemann, U.; Timm, O.;
766 Timmermann, A.;Toggweiler, J.R. (2007), Modulation of the bipolar seesaw in the Southeast
767 Pacific during Termination 1, Earth Planet. Sci. Lett. 259, 400–413, doi:
768 10.1016/j.epsl.2007.04.040.

Mahowald, N. M. and Kiehl, L. M. (2003), Mineral aerosol and cloud interactions, Geophys. Res. Lett., 30, 1475, doi:10.1029/2002GL016762.

Mahowald, N.; Albani, S.; Engelstaedter, S.; Winckler, G. and Goman, M. (2011), Model insight into glacialeinterglacial paleodust records, Quat. Sc. Rev. 30, 832 – 854, doi:10.1016/j.quascirev. 2010.09.007.

Marino, F., Castellano, E., Nava, S., Chiari, M., Ruth, U., Wegner, A., Lucarelli, F., Udisti, R., Delmonte, B., and Maggi, V. (2009), Coherent composition of glacial dust on opposite sides of the East Antarctic Plateau inferred from the deep EPICA ice cores, Geophys. Res. Lett., 36, L23703, doi:10.1029/2009GL040732.

Martínez-Garcia, A.; Rosell-Melé, A.; Geibert, W. (2009), Gersonde, R.; Masqué, P.; Gaspari and Barbante, C.: Links between iron supply, marine productivity, sea surface temperature, and CO_2 over the last 1.1 Ma, Paleoceanography, 24, PA1207, doi: 10.1029/2008PA001657.

Masson-Delmotte, V.; Jouzel, J.; Landais, A.; Stievenard, M.; Johnsen, S.; White, J.; Werner, M.; Sveinbjornsdottir, A. & Fuhrer, K. (2005) GRIP Deuterium Excess Reveals Rapid and Orbital-Scale Changes in Greenland Moisture Origin, Science, 309, 118-121, doi: 10.1126/science.1108575.

McConnell J.R., Aristarain A.J., Banta J.R., Edwards P.R. and Simoes J.C. (2007), 20th-Century doubling in dust archived in an Antarctic Peninsula ice core parallels climate change and desertification in South America. PNAS 104(14):5743–5748, 10.1073/pnas.0607657104.

795 Petit, J.R. and Delmonte, B. (2009), A model for large glacial–interglacial climate-induced
796 changes in dust and sea salt concentrations in deep ice cores (central Antarctica):
797 palaeoclimatic implications and prospects for refining ice core chronologies, Tellus, 61B,
798 768-790, doi: 10.1111/j.1600-0889.2009.00437.x
799
800 Petit, J. R.; Jouzel, J.; Raynaud, D.; Barkov, N. I.; Barnola, J. M.; Basile, I.; Benders, M.;
801 Chappellaz, J.; Davis, M.; Delaygue, G.; Delmotte, M.; Kotlyakov, V.; Legrand, M.;
802 Lipenkov, V. Y.; Lorius, C.; Pepin, L.; Ritz, C.; Saltzman, E. and Stievenardt, M.
803 (1999), Climate and atmospheric history of the past 420 000 years from the Vostok ice core,
804 Antarctica, Nature, 399, 429 – 436, doi: 10.1038/20859.
805
806 Reijmer, C.H. and van den Broeke, M. R. (2001), Moisture source of precipitation in Western
807 Dronning Maud Land, Antarctica, Antarctic Science, 13(2), 210-220.
808
809 Reijmer, C. H., van den Broeke, M. R., and Scheele, M. P. (2002), Air parcel trajectories to
810 five deep drilling locations on Antarctica, based on the ERA-15 data set. J. Climate 15, 1957-
811 1968.
812
813 Revel-Rolland, M., De Deckker, P., Delmonte, B., Hesse, P. P., Magee, J. W., Basile-
814 Doelsch, I., Grousset, F., and Bosch, D. (2006), Eastern Australia: A possible source of dust
815 in East Antarctica interglacial ice, Earth Planet. Sc. Lett., 249, 1–13,
816 doi:10.1016/j.epsl.2006.06.028.
817
818 Röthlisberger, R., Bigler, M., Hutterli, M., Sommer, S., Stauffer, B., Junghans, H. G., and
819 Wagenbach, D. (2000), Technique for continuous high-resolution analysis of trace substances
820 in firn and ice cores, Environ. Sci. Technol., 34, 338–342, doi: 0.1021/es9907055.

821

822 Röthlisberger, R., Mulvaney, R.,Wolff, E.W., Hutterli, M. A., Bigler, M., Sommer, S., and
823 Jouzel, J. (2002), Dust and sea salt variability in central East Antarctica (Dome C) over the
824 last 45 kyrs and its implications for southern high-latitude climate, Geophys. Res. Lett., 29,
825 1963, doi:10.1029/2002GL015186.

826

827 Ruth, U.; Wagenbach, D.; Steffensen, J. P. and Bigler, M. (2003), Continuous record of
828 microparticle concentration and size distribution in the central Greenland NGRIP ice core
829 during the last glacial period, J. Geophys. Res., 108, doi:10.1029/2002JD002376.

830

831 Schlosser, E.; Manning, K.W.; Powers, J.G.; Duda, M.G.; Birnbaum, G. and K. Fujita, K.
832 (2010), Characteristics of high-precipitation events in Dronning Maud Land, Antarctica, J.
833 Geophys. Res., 115, D14107, doi:10.1029/2009JD013410.

834

835 Sommer, S.; Wagenbach, D.; Mulvaney, R. and Fischer, H. (2000), Glacio-chemical study
836 spanning the past 2 kyr on three ice cores from Dronning Maud Land, Antarctica 2.
837 Seasonally resolved chemical records, J. Geophys. Res., 105, D24, 29423-29433, doi:
838 10.1029/2000JD900450.

839

840 Stenni, B.; Buiron, D.; Frezzotti, M.; Albani, S.; Barbante, C.; Bard, E.; Barnola,M., Baroni,
841 M.; Baumgartner, M.; Bonazza, M.; Capron, E.; Castellano, E.; Chappellaz, J.; Delmonte, B.;
842 Falourd, S.; Genoni, L.; Iacumin, P.; Jouzel, J.; Kipfstuhl, S.; Landais,S.; Lemieux-Dudon, B.;
843 Maggi, V.; Masson-Delmotte, V.; Mazzola, C.; Minster, B.; Montagnat, M.; Mulvaney, R.;
844 Narcisi,B.; Oerter, H.; Parrenin, F.; Petit, J. R.; Ritz, C.; Scarchilli, C.; Schilt, A.; Schüpbach,
845 S.; Schwander, J.; Selmo E.; Severi, M.; Stocker, T. F. and Udisti, R. (2010), Expression of

the bipolar see-saw in Antarcticclimate records during the last deglaciation, Nat Geoscience 4, 46–49, doi:10.1038/ngeo1026.

Tuncel, G.; Aras, N.K.; Zoller, W.H. (1989), Temporal variations and sources of elements in the Southpole atmosphere: 1. nonenriched and moderately enriched elements, J. Geophys. Res., 94, D10, 13025-13039.

Unnerstad, L. and Hansson, M. (2001), Simulated airborne particle size distributions over Greenland during Last Glacial Maximum, Geophys. Res. Lett., 28 (2), 287-290, 10.1029/2000GL012194.

Veres, D., Bazin, L., Landais, A., Lemieux-Dudon, B., Parrenin, F., Martinerie, P., Toye Mahamadou Kele, H., Capron, E., Chappellaz, J., Rasmussen, S., Severi, M., Svensson, A., Vinther, B., and Wolff, E. (2013), The Antarctic ice core chronology (AICC2012): an optimized multi-parameter and multi-site dating approach for the last 120 thousand years, Climate of the Past, 1733-1748, doi:10.5194/cp-9-1733-2013.

Wegner, A.; Gabrielli, P, Wilhelms-Dick, D., Ruth, U., Kriews, M., De Deckker, P., Barbante, C., Cozzi, G., Delmonte, B. and Fischer, H. (2012), Change in dust variability in the Atlantic Sector of Antarctica at the end of the last deglaciation, Clim.Past, 8, 135-147, 10.5194/cp-8-135-2012.

Weller R. and Wagenbach, D. (2007) Year-round chemical aerosol records in continental Antarctica obtained by automatic samplings, Tellus, 59B, 755–765 doi: 10.1111/j.1600-0889.2007.00293.x.

872 Welker, C., Martius, O., P., F., Reijmer, C. H., and Fischer, H. (2015), A climatological
873 analysis of high-precipitation events in Dronning Maud Land, Antarctica, and associated
874 large-scale atmospheric conditions, J Geophys Res, 119, 11,932–911,954,
875 10.1002/2014JD022259.
876

877 **Figures**

878

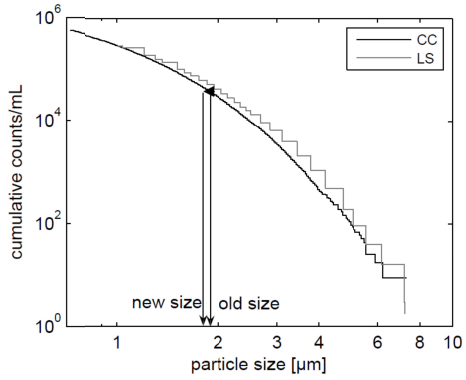

879

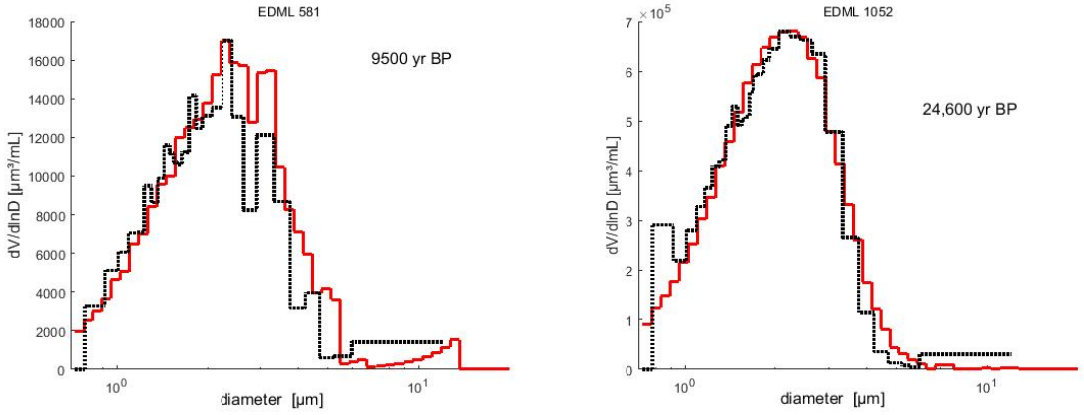

880 Figure 1: Illustration of the calibration method: The LPD size spectrum (LS) is shifted onto
881 the CC spectrum to obtain new bin sizes (top). Examples for the size distribution used for the
882 calibration from the Holocene (~9500 yr BP, left) and Glacial (~24,500 yr BP, right). The
883 LPD data are shown after the adjustment of the size axis and averaging the 45 individual
884 calibration lines. CC data are shown in red, LPD data are shown in black. Note, that
885 especially the maximum in the size distribution, which is always at a diameter close to 2 µm,
886 is practically identical for both methods after recalibration.

887

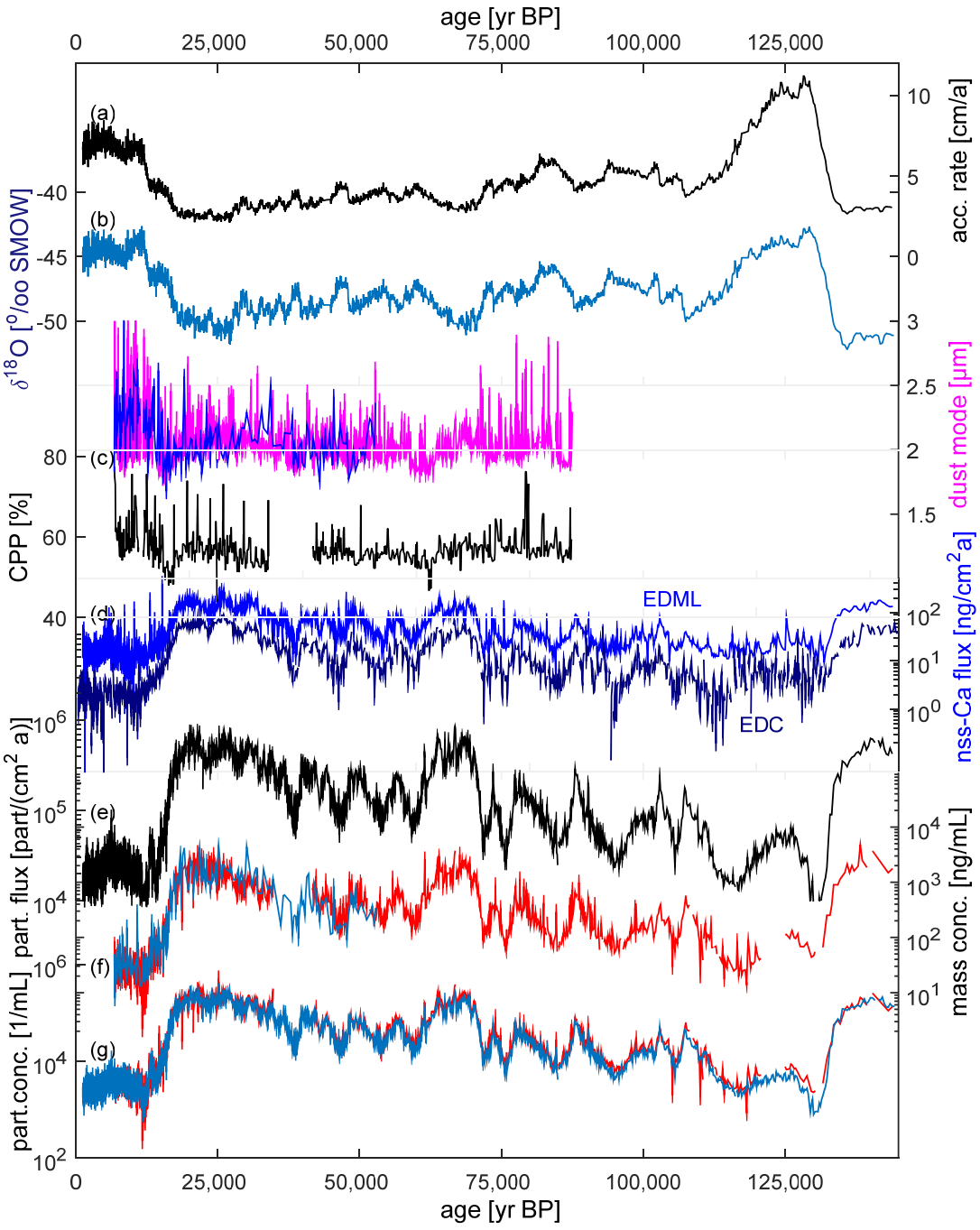

888

889

890 Figure 2:

891 Overview over the EDML dust record: (a) accumulation rates derived from $\delta^{18}O$ (EPICA-

892 community members, 2006], (b) $\delta^{18}O$ EPICA-community members, 2006], (c) dust size in

893 terms of coarse particle percentage (CPP, ratio of mass of particles larger than 2 µm with

894 respect to total mass, black), modal value of the volume distribution derived from
895 measurements using the LPD (magenta) and CC (blue) (all this study), (d) nss-Ca flux from
896 EDML (light blue) and EDC (dark blue, both [Kaufmann et al. 2010]), (e) dust particle flux
897 (this study), (f) dust mass concentration (this study), and (g) dust particle concentration (this
898 study).
899
900

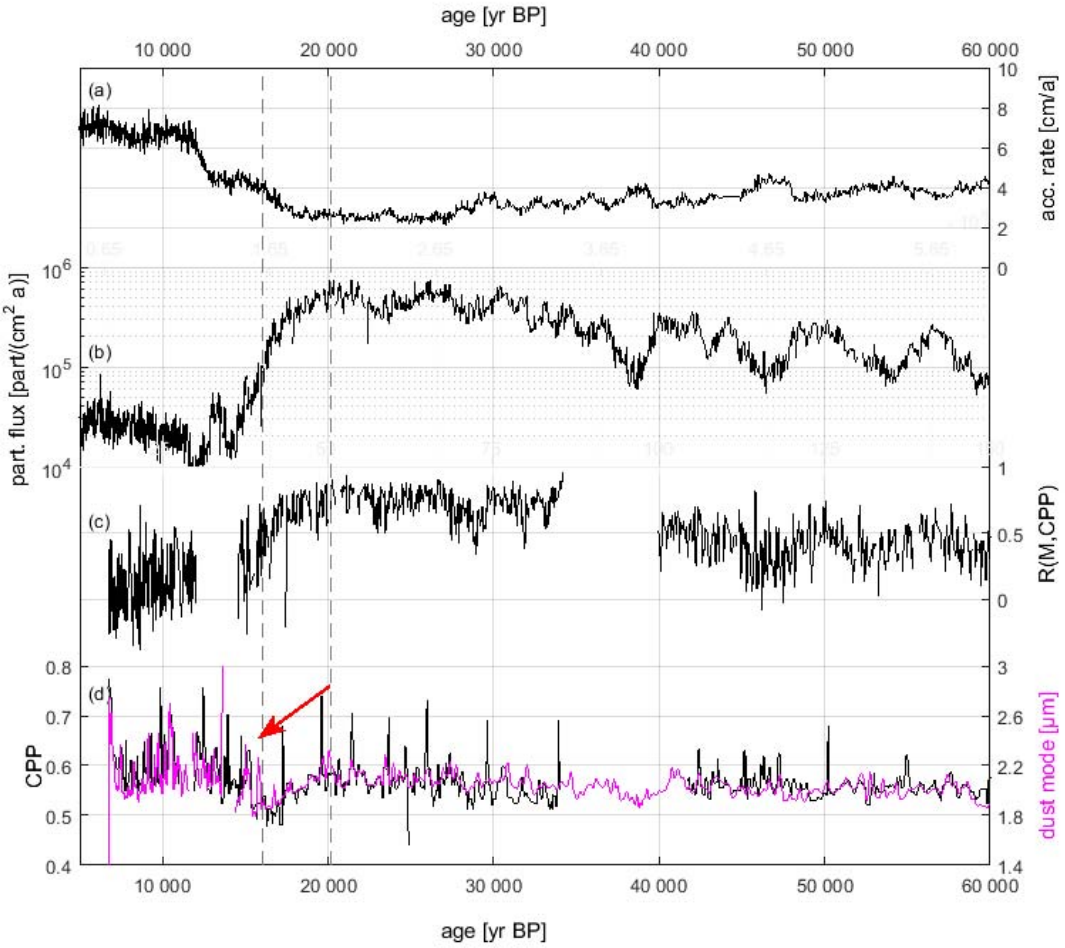

901

902 Figure 3:

903 Overview of dust characteristics in EDML during Transition I: (a) accumulation rates derived
904 from $\delta^{18}O$ [EPICA-community members, 2006], (b) dust particle flux, (c) correlation
905 coefficient between dust mass and dust size and (d) dust size in terms of CPP (black) and dust
906 mode (magenta). The red arrow indicates the decrease in dust size between 20,000 yr BP and
907 16,000 yr BP before the dust size increases again at 16,000 yr BP

908

909

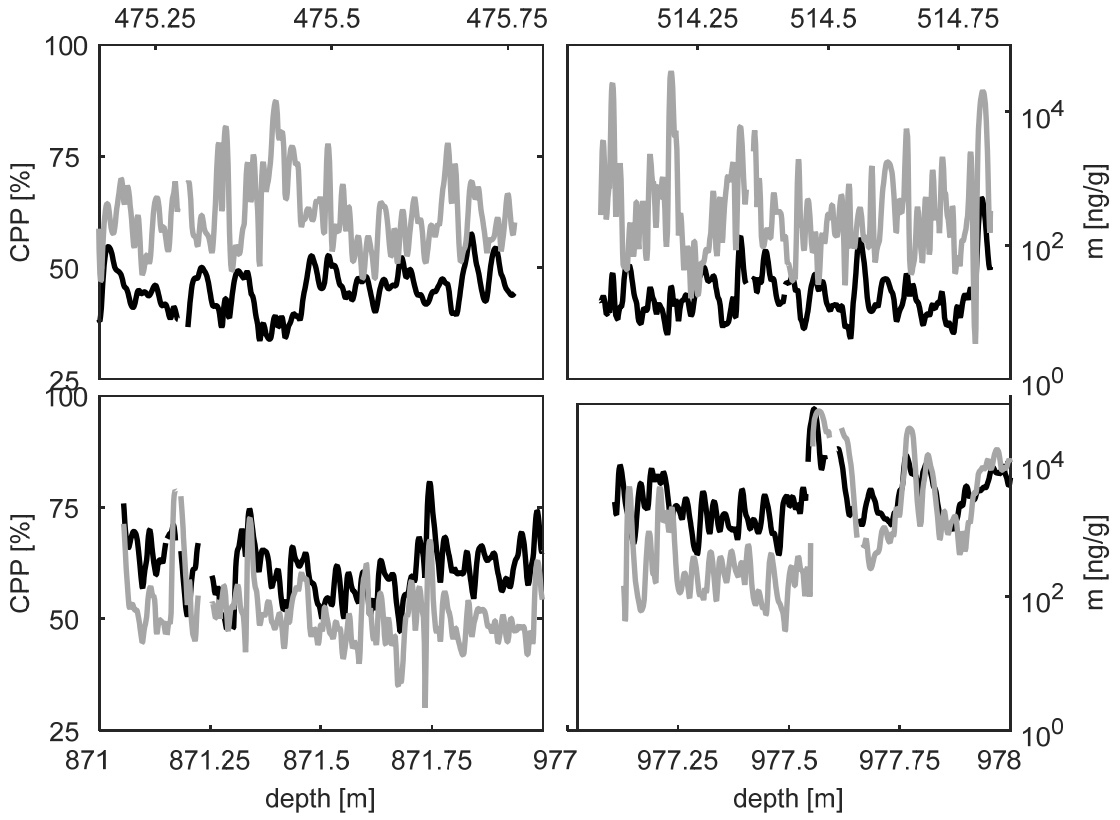

Figure 4:

Four examples for size (given in coarse particle percentage CPP, grey) and dust mass concentration (black line) in different climatic stages. Holocene (2 upper examples, ~7200 yr BP and ~8000 yr BP), transition (lower left ~17,000 yr BP) and LGM (lower right, ~21,400 yr BP). The y-axes are the same in all subfigures. The correlation between concentration and size is higher during the LGM than during the Holocene.

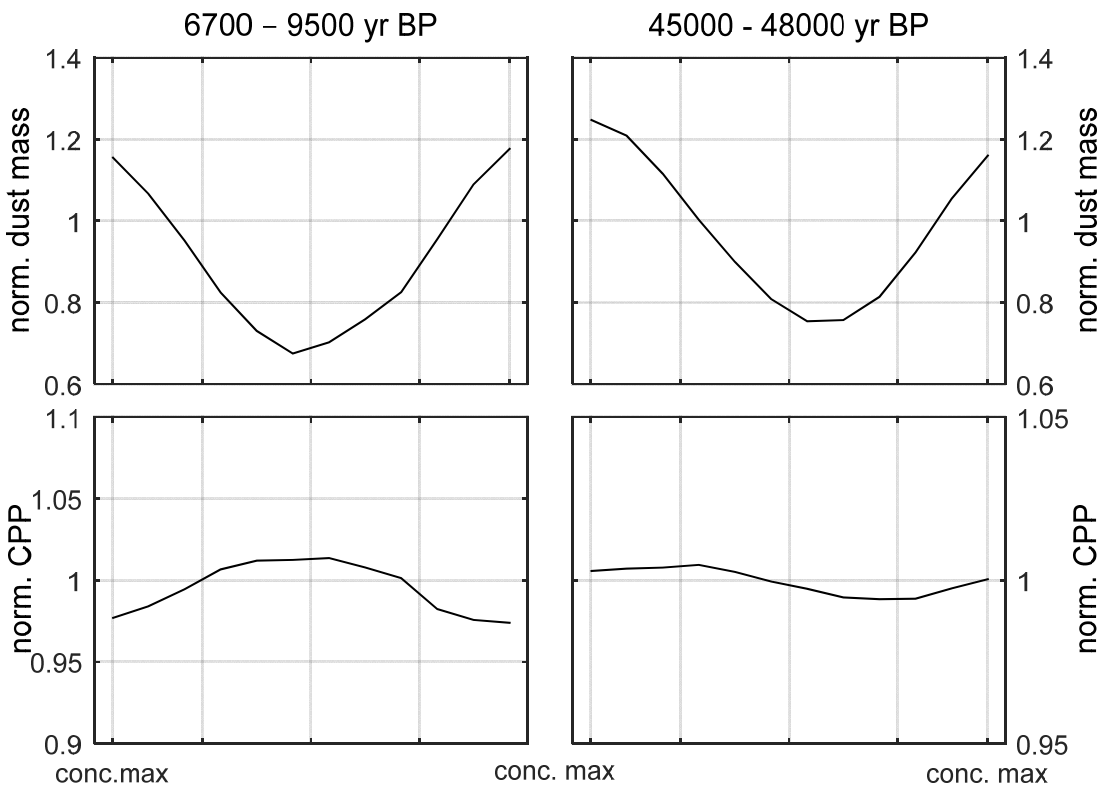

Figure 5:

Relative seasonality of dust concentration (top) and size (bottom during the Holocene (left) and the Glacial (right): The median of the normalized seasonal cycle of dust mass and concentration was calculated. 12 time steps over one year are linear interpolated within one year according to the annual layer counted year based on the ammonium concentration peak. During recent times the dust concentration maximum occurs during winter *[Sommer et al. 2000*]. We assume that the dust concentration maximum also occurs during winter during the time intervals presented here.

927

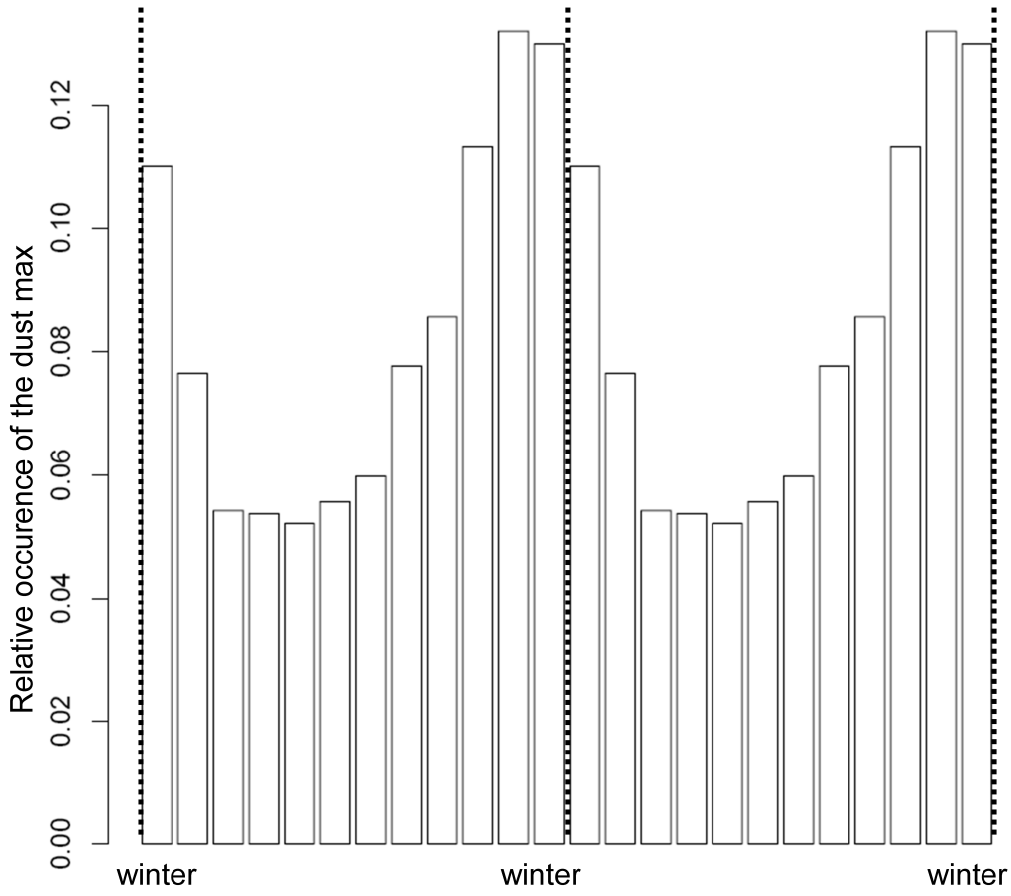

928

929 Figure 6:

930 Histogram of the seasonal occurrence of the dust maxima atEDML relative to the Na^{+}-
931 concentration maximum in winter. The dashed lines indicate the maximum of the Na+-
932 concentration over the Holocene (~2000 yr BP – ~15,000 yr BP). Thedust peak occurs twice
933 as likely in winter than in summer.

934

935

936

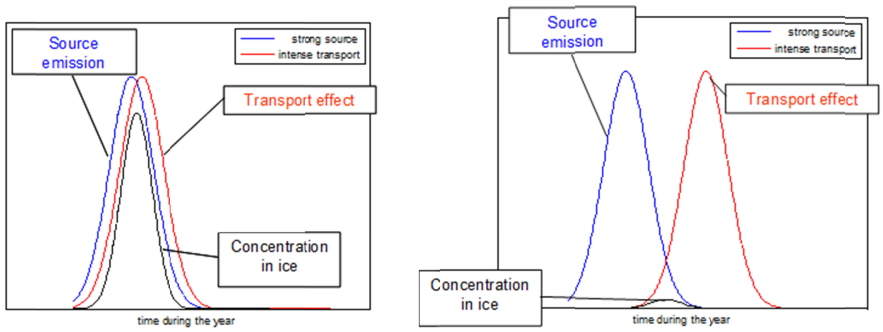

Figure 7:

Illustration of the conceptual model for the phasing of dust transport and source emission strength. Maximum dust emission and maximum transport intensity occur simultaneously during the year (left) as is the case during glacial conditions. A phase shift between the two effects results in a significantly lower dust concentration in the ice (right).

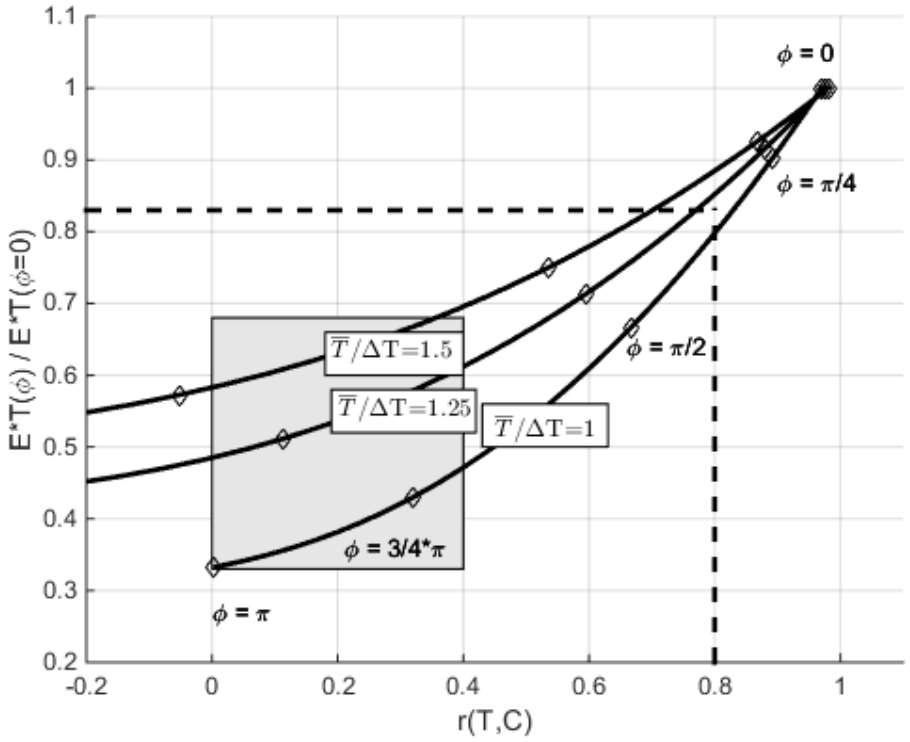

Figure 8:

Product of transport efficiency T and source emission strength E (E*T(φ))/(E*T(φ=0)) vs. correlation coefficient r between dust concentration in the ice core C and transport intensity T for different φ and different $\bar{T}/\Delta T$ (Equation 4). This figure illustrates the reduction of dust in the ice due to a phase shift between maximum transport efficiency and the maximum of source emission strength. The dashed lines illustrate the mean correlation coefficient of CPP and dust concentration during the Glacial. The grey square gives the range of respective correlation coefficients during the Holocene.

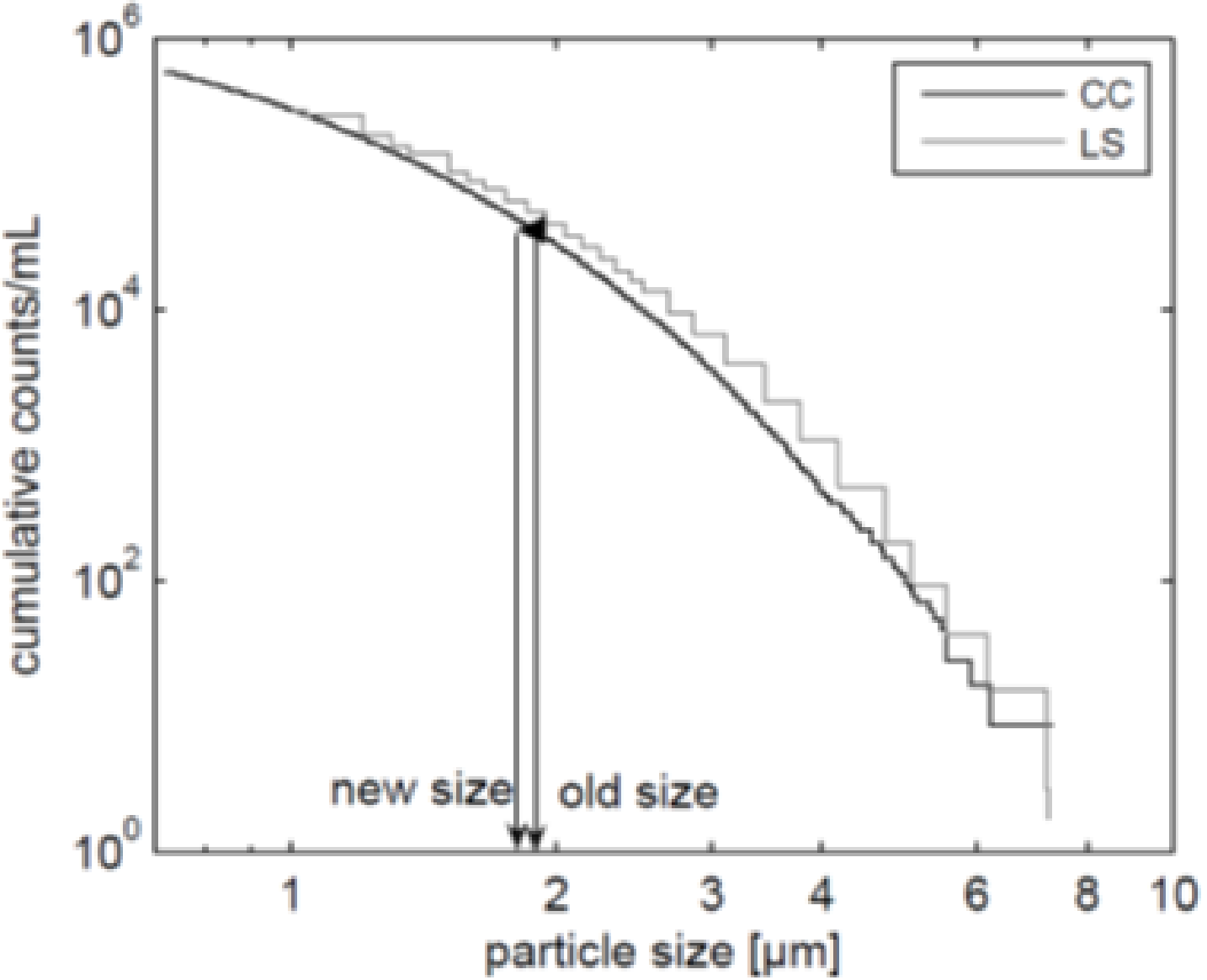
CC
LS
cumulative counts/mL
10^6
10^4
10^2
10^0
new size
old size
1
2
3
4
6
8
10
particle size [µm]

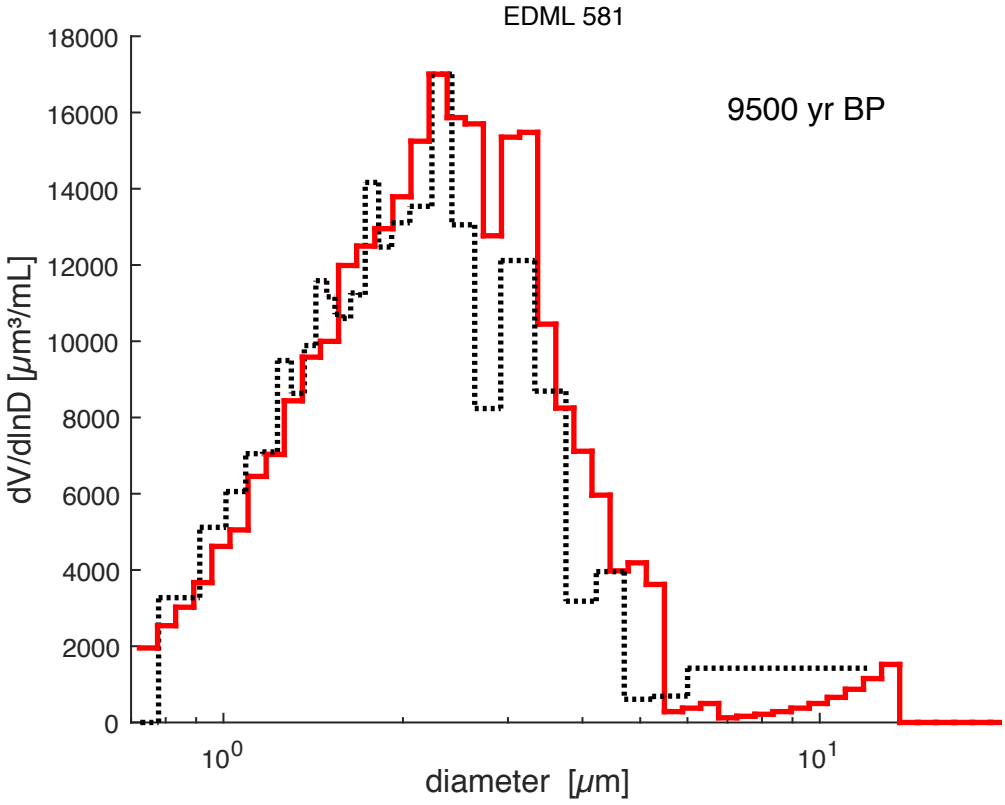
EDML 581
9500 yr BP
18000
16000
14000
12000
10000
8000
6000
4000
2000
0
dV/dlnD [μm³/mL]
10^0
10^1
diameter [μm]

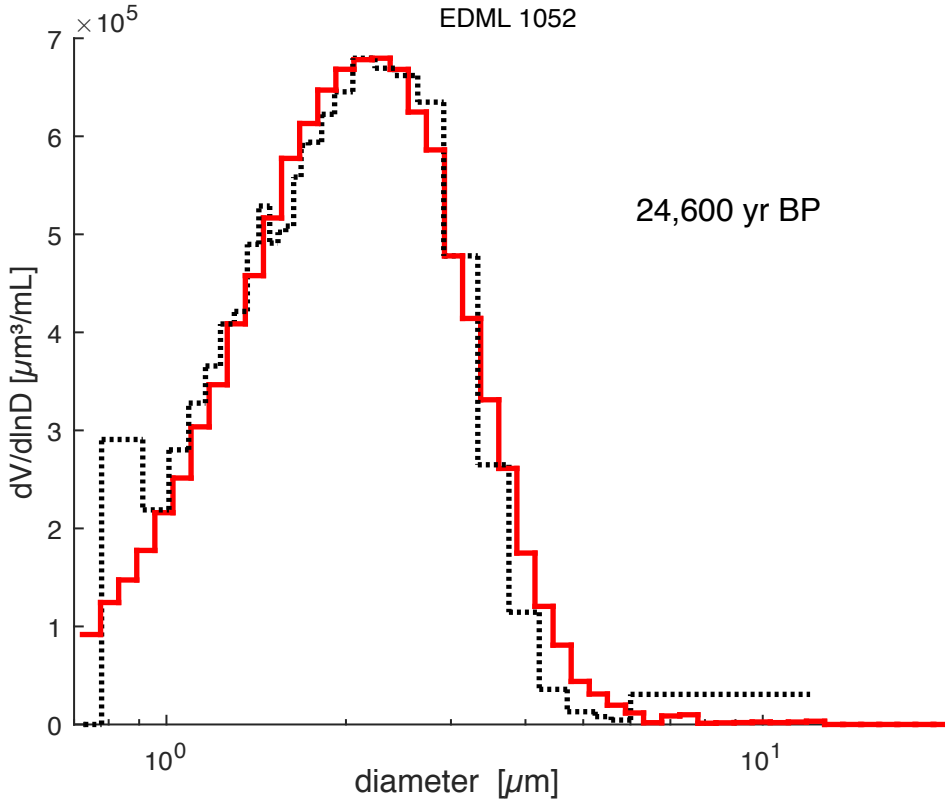
EDML 1052
×10^5
7
6
5
4
3
2
1
0
dV/dlnD [μm³/mL]
24,600 yr BP
10^0
10^1
diameter [μm]

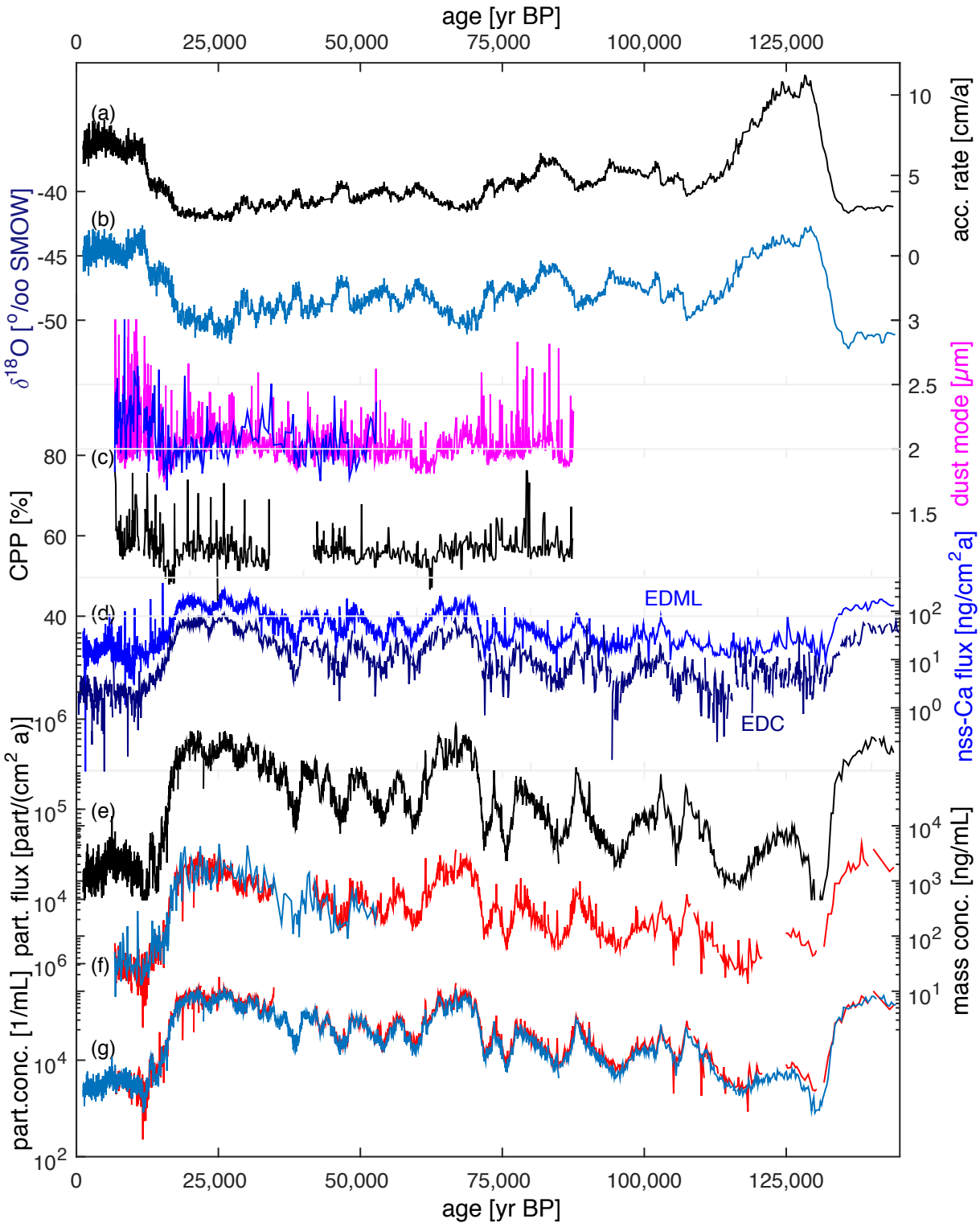
age [yr BP]
0
25,000
50,000
75,000
100,000
125,000
(a)
(b)
(c)
(d)
(e)
(f)
(g)
δ18O [o/oo SMOW]
-40
-45
-50
acc. rate [cm/a]
10
5
0
CPP [%]
80
60
40
dust mode [μm]
3
2.5
2
1.5
EDML
EDC
nss-Ca flux [ng/cm2a]
10^2
10^1
10^0
part. flux [part/(cm2 a)]
10^6
10^5
10^4
part.conc. [1/mL]
10^6
10^4
10^2
mass conc. [ng/mL]
10^4
10^3
10^2
10^1

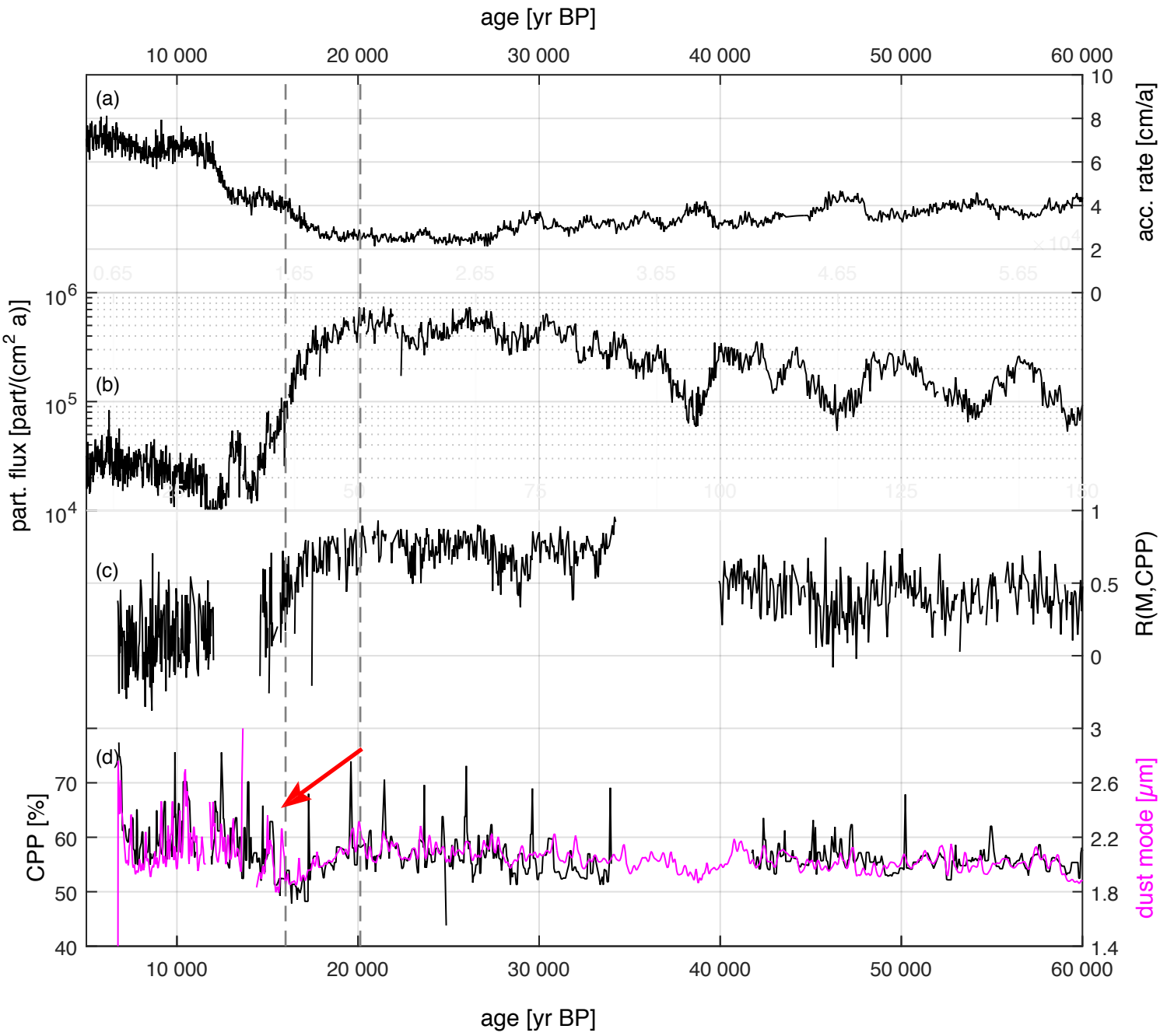
age [yr BP]
10 000
20 000
30 000
40 000
50 000
60 000
(a)
(b)
(c)
(d)
acc. rate [cm/a]
part. flux [part/(cm^2 a)]
10^6
10^5
10^4
R(M,CPP)
CPP [%]
dust mode [μm]
70
60
50
40
3
2.6
2.2
1.8
1.4
1
0.5
0
10
8
6
4
2
0
age [yr BP]

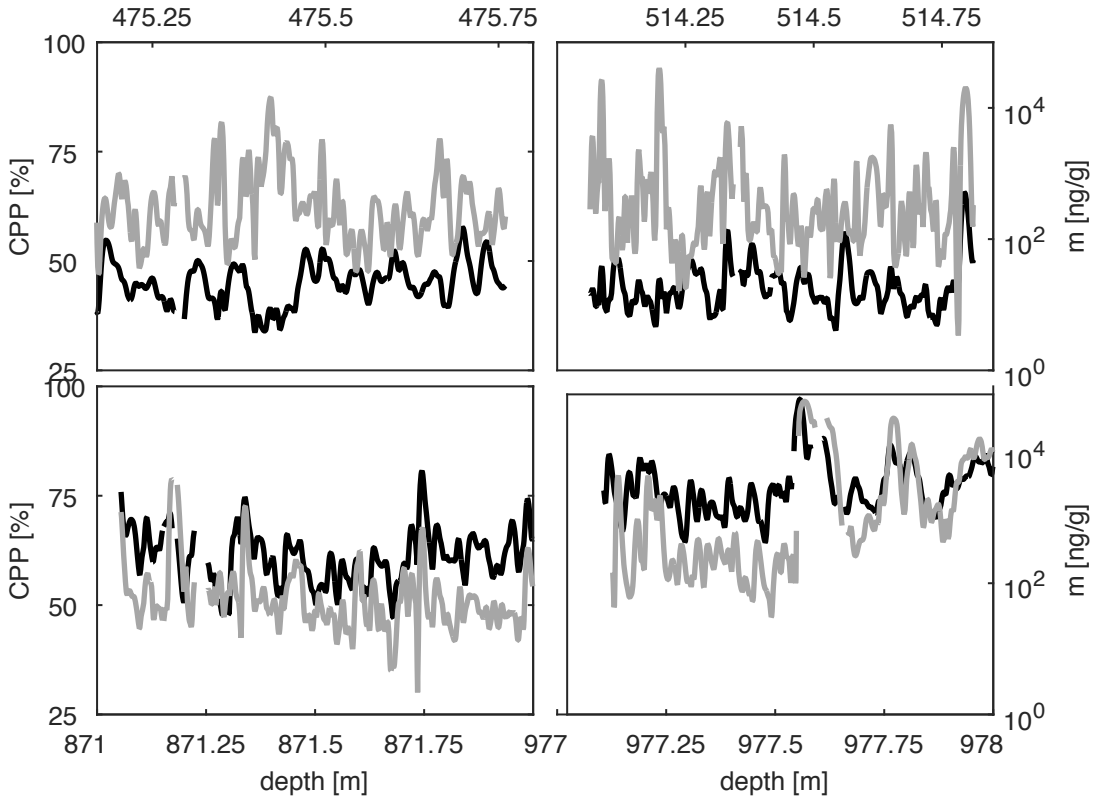
475.25
475.5
475.75
514.25
514.5
514.75
100
75
50
25
CPP [%]
10^4
10^2
10^0
m [ng/g]
871
871.25
871.5
871.75
977
977.25
977.5
977.75
978
depth [m]

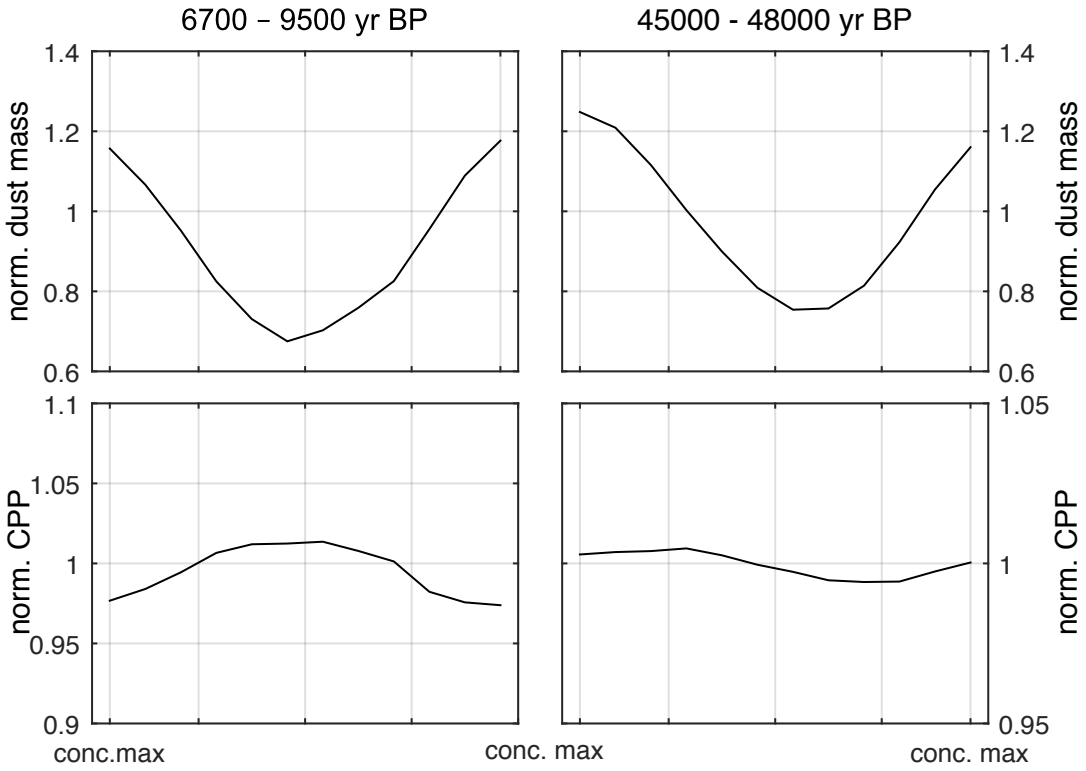
6700 – 9500 yr BP
45000 - 48000 yr BP
norm. dust mass
norm. CPP
1.4
1.2
1
0.8
0.6
1.1
1.05
0.95
0.9
conc.max
conc. max
conc. max

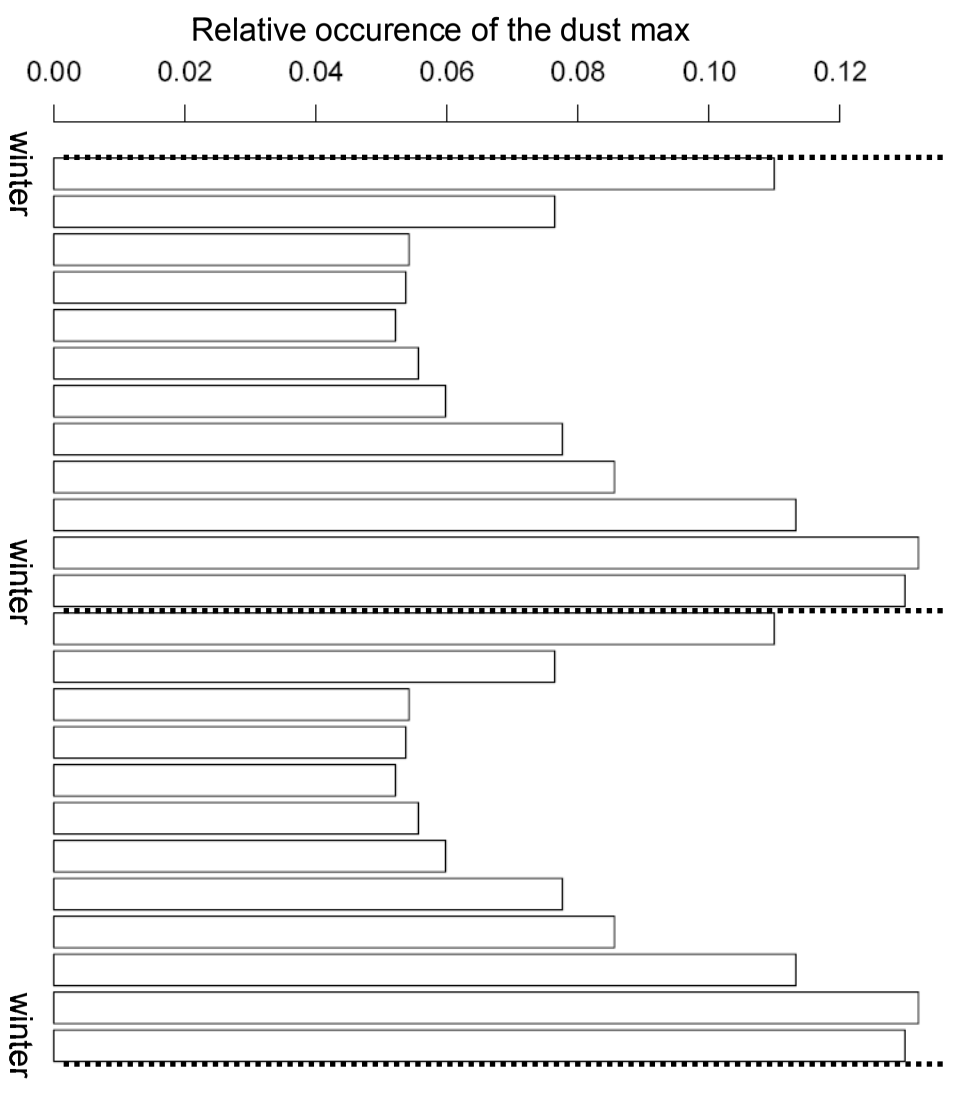
Relative occurence of the dust max
0.00
0.02
0.04
0.06
0.08
0.10
0.12
winter
winter
winter

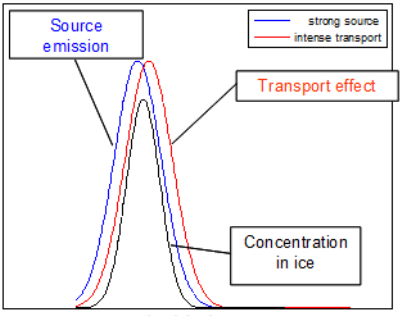
Source emission
strong source
intense transport
Transport effect
Concentration in ice
time during the year

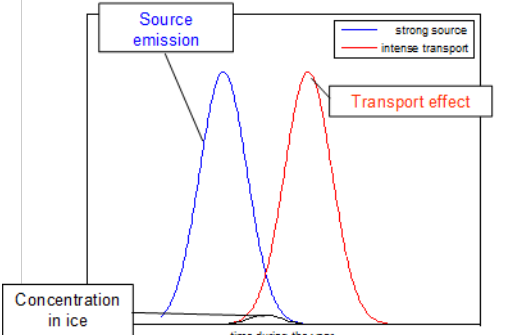
Source emission
strong source
intense transport
Transport effect
Concentration in ice
time during the year

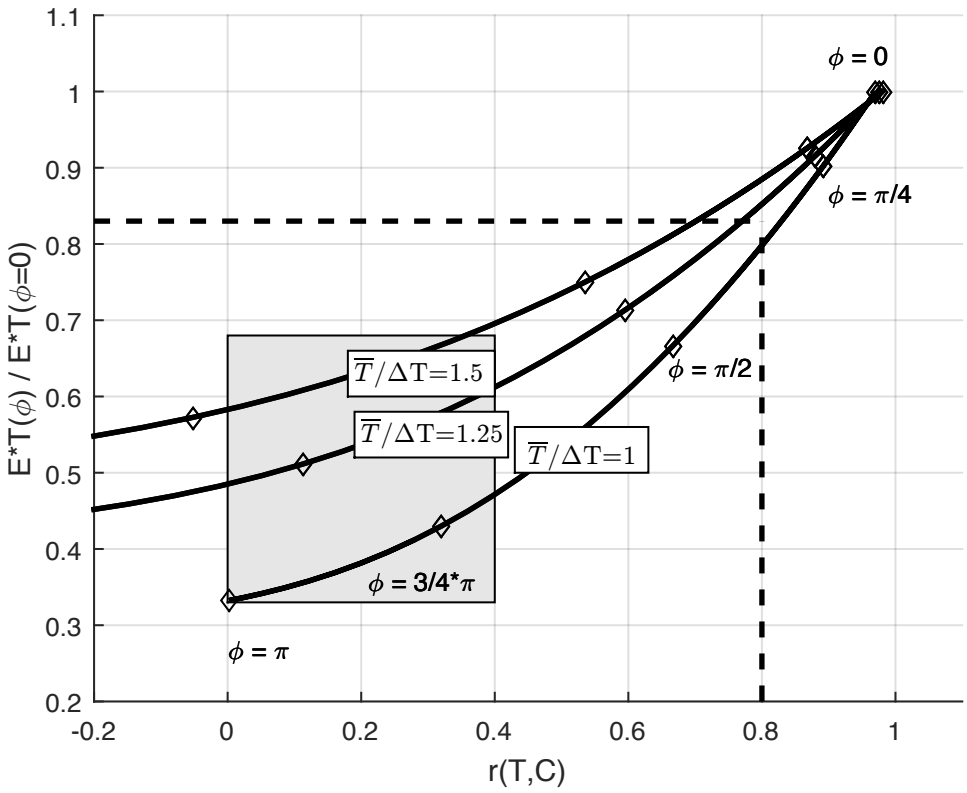
1.1
1
0.9
0.8
0.7
0.6
0.5
0.4
0.3
0.2
-0.2
0
0.2
0.4
0.6
0.8
1
E*T(ϕ) / E*T(ϕ=0)
r(T,C)
ϕ = 0
ϕ = π/4
ϕ = π/2
ϕ = 3/4*π
ϕ = π
$\overline{T}/\Delta T=1.5$
$\overline{T}/\Delta T=1.25$
$\overline{T}/\Delta T=1$